

**UCSF**

**UC San Francisco Electronic Theses and Dissertations**

**Title**

Multifaceted roles of the lipid scramblase TMEM16F in tauopathy

**Permalink**

<https://escholarship.org/uc/item/68n7c2dk>

**Author**

Zubia, Mario Victor

**Publication Date**

2021

Peer reviewed|Thesis/dissertation

Multifaceted roles of the lipid scramblase TMEM16F in tauopathy


by  
Mario Victor Zubia

DISSERTATION  
Submitted in partial satisfaction of the requirements for degree of  
DOCTOR OF PHILOSOPHY

in  
Biomedical Sciences


in the  
GRADUATE DIVISION  
of the  
UNIVERSITY OF CALIFORNIA, SAN FRANCISCO

Approved:

DocuSigned by:  
  
9A805C3F0428410... Eric Huang  
Chair

DocuSigned by:  
  
Lily Jan

DocuSigned by:  
  
Clifford Lowell

DocuSigned by:  
  
F69F10B7A1234BF... Mary Nakamura

Committee Members

Copyright 2021

By

Mario Victor Zubia

*This dissertation is dedicated to mom  
without whose guidance and support, none of this would have been possible*

## **Acknowledgements**

As cliché as it sounds, it really does take a village. It has been a long and arduous journey, but so many people have come along and have been there at every step of the way. I would first and foremost like to thank my thesis advisor, Lily Jan, and Yuh Nung Jan, who have been so instrumental in their support throughout my PhD. They have provided immense resources and guidance, while allowing me to become the independent and critical scientist I am today. Lily has given me the independence to establish my own project, the independence to fail, and the independence to succeed. While extremely overwhelming at times, I am now so thankful to have developed this critical skillset as I move forward in my scientific journey. Apart from independence, Lily has always been there to provide insight or suggest hypotheses that sounded crazy at the time but ended up being completely correct, of which I am still in awe. She has always been patient and warm and kind. When experiments did not go as planned, or I had to start anew, her demeanor let me know that it was all going to be okay. I am grateful to her and some day, I hope to be an echelon of the scientist she is.

I would also like to acknowledge my thesis committee members Mary Nakamura and Clifford Lowell, and especially my chair Eric Huang for their invaluable feedback and guidance. When established my thesis committee, I was studying platelets in arthritis—very far removed from this current work. Despite the major shift to neurodegeneration, they have been able to provide amazing suggestions and I am so grateful to have gotten their insight. Eric has been a pivotal part of my success. Over the last few years, I have picked the brain of many Huang lab members and now perform all my DAB histology in his lab; stains that used to fail miserably, now work perfectly. His support and help analyzing data pushed my project forward. In addition to my thesis committee, I would like to thank my other scientific mentors including Li Gan and Susanna Rosi. I performed laboratory rotations in both labs and throughout my PhD, I was constantly picking their brains on microglia and neuroinflammation. Additionally, Susanna has been a strong pillar of support. Learning about her journey into science and how it related to

mine really made me feel at home when we spoke, and her motivation helped propel me forward. Eric, Susanna, and Li also all provided letters of recommendations for many of my grant applications including my awarded NIH F99 grant, upon which I am so very thankful.

Thank you to the past and present BMS program administration staff Lisa Magargal, Demian Sainz, Monique Piazza, Nate Jew, and Ned Molyneaux, who helped make my experience with classes, stipends, journal clubs, and other graduate program issues seamless. You all allow BMS to run extremely smoothly and this one less worry is very comforting.

The bulk of my PhD experience actually came down to the day to day, and for that, I have countless members of the Jan lab to thank. Staring from when I first rotated, Chin Fen Teo, you were a great mentor and continue to be an amazing resource to all things everything. Thank you to Andrew Kim for helping me get started with TMEM16F and teaching me flow cytometry. You helped advance my study of TMEM16F in microglia and I'm very thankful for all the guidance you provided. Sarah Headland, you were instrumental in helping me pass qualifying exam. I had to learn about arthritis and platelets from scratch and your expertise and support was crucial to my success. Tina Han, for these last few years, you have been one of my biggest sources of support and a constant sounding board for experiments. I honestly think that without your guidance, I would still be struggling with imaging or troubleshooting all of my molecular cloning. Thank you so, so much. Adeline Yong, your arrival to the lab could not have come at a better time. I am grateful for your help with my neuronal cultures. My project, though still not complete, would be so far away from where it is today without your magic trituration hands. And to my other former and current Jan lab members and friends in no particular order including but not limited to: Jason Tien, Christian Peters, Mu He, Ke Li, Shengjie Feng, Beverly Piggott, Caitlin O'Brien, Han-Hsuan Liu, Maja Petkovic, Jacob Jaszczak, David Crottes, Marena Tynan-La Fontaine, Cherlye Xiang, and Laura DeVault, thank you for being there to talk, chat, discuss random things like putting forks in the microwave, and share memes in the lunchroom. You made coming to lab a much happier, better place.

I am also thankful to two other lab members, fellow classmates, and some of my closest friends, Hung Lin and Lynn Wang. Honestly, I have no idea how I would have survived lab without you two. You were my moral support and we have been able to commiserate during failures and celebrate during successes. Along with John King, Faten Sayed, and eventually Lay Kodama, I am so glad to have met you all and that we were able to share so much delicious food, cute dogs, and adventures together. Grad school without you would have been much worse and I am so privileged to have you as friends.

To my friends from the BMS program, Briana Fitch, KT Nguyen, Christina Abundis, and Berky Gebrekristos, thank you for helping me feel at home in San Francisco. When I first came to grad school, I felt lost, but spending time with the “Mission Bay Crew” and having our infamous cooking nights, dinners around the city, or nights out on the town was a great source of belonging for me. I cannot stress enough how important this was for me to feel welcome. I am so proud to see what all of you have accomplished and I am grateful to have shared so many experiences together.

And to my Caltech friends, I am extremely lucky to still have your support: Steven Okai, Kelvin Fang, Melissa Xu, Kristen Holtz, Sabrina Sun, Yifei Huang, Sandhya Chandrasekeran, Ahalaya Prabakar, Joel Xu, Seorim Song, Tim MacDonald, and Shir Aharon. Our group chat has kept the best part of college alive and it has been so helpful to hear each other’s struggles and successes in grad school and in life. Our lunches, celebrations, vacations, and hangouts have been so enjoyable, and have really helped me keep a positive attitude during the ups and downs of grad school. To my UCSF/ SF Caltech friends Megan Lo, Alex Yeh, Stephany Lai, and Jon Schor, thank you for the food, talks, and desserts. I was always able to count on you to accompany me to try a new restaurant or dessert spot, or provide an ear for me to complain about a failed experiment. I am very thankful for having you with me during the last many years.

Apart from those directly involved in my graduate school experience, I would like to thank my scientific mentors leading up to UCSF. Thank you to my undergraduate advisors

Bruce Hay and Paul Patterson. Bruce, thank you so much for letting me, a lowly freshman with no lab experience whatsoever, begin my scientific journey. With support from you, Kelly Dusingberre, and Omar Akbari, I began to understand how to design and perform experiments. Your enthusiasm and support for me, even if I failed, was extremely helpful. My work with Paul allowed me to develop my love of neuroinflammation. Jan Ko, you were so caring, and I am so thankful for all the support you provided in lab. I would also like to thank Ali Khoshnan, who helped push me to design better experiments and be more critical when analyzing data.

Going further back, thank you to my second, third, and fourth/ fifth grade teachers Mrs. Hanewich, Mr. Belding, and Mrs. Webb. Growing up, I knew no scientists, had no idea what research was, and could count the number of college-educated people I knew on one hand. You three helped to foster my love of math and science and really helped me to believe in myself and my abilities.

To my biggest supporters, my family, thank you for your continued, unwavering support. Looking back, I realize I have been pretty absent throughout college and graduate school, but you have always been there for me—every graduation, every birthday, every anything. I am so thankful to have such amazing and loving sisters, Veronica, Senia, Kassie; a munchkin niece, Ava and now nephew, Zach; and my biggest champion and advocate, mom. Mom—Mother Nature—I know we do not always see eye-to-eye on everything, but your continued support has enabled me to accomplish this wonderful feat. All my hard work is for you. You have given us kids the motivation to do well and I want you to know your struggles and hardships have not been in vain. I am thankful for all the nonstop rides to early-morning or late-night classes, perpetual chaperoning and volunteering, the resulting lack of sleep, and the thousands of other things you did to give us a wonderful upbringing. With my PhD, know your hard work, love, and support has paid off.

Finally, I would like to acknowledge my Grandma Nellie, who we officially lost to her struggle with Alzheimer's disease in 2015. Unofficially, however, we lost her in 2005, when the



bubbly and happy woman I grew up with, was no more. Seeing how the disease slowly stripped her away from us and the immense pain it caused helped invigorate my passion into understanding biology and further motivated me to pursue biomedical sciences and eventually neuroscience. My grandma always told me I could do whatever I set my mind to, so Grandma Nellie, I hope my studies into neurodegeneration can someday help others prevent the loss we experienced with you.

## **Contributions**

The work described in this dissertation was performed under the direct supervision and guidance of Lily Yeh Jan, with the support of Yuh Nung Jan and Eric Huang, my thesis committee chair. All chromogenic immunohistochemistry was performed using resources in the lab of Eric Huang. Mouse behavioral experiments and their initial statistical analyses were performed by the Gladstone Institute for Disease Behavioral Core. Survival of primary neuronal cultures for use in *in vitro* assays would not have been possible without direct support from Adeline Yong. Additional guidance and insights were provided by Tina Han and my remaining thesis committee members: Clifford Lowell and Mary Nakamura. Data from chapters 2 and 3 are unpublished, but in preparation for submission.

## Multifaceted roles of the lipid scramblase TMEM16F in tauopathy

Mario Victor Zubia

### ABSTRACT

TMEM16F is a calcium-activated phospholipid scramblase and non-selective ion channel, which can move lipids bidirectionally across the plasma membrane. While earliest studies of TMEM16F have implicated its function in the release of microvesicles, large extracellular vesicles budded directly from the plasma membrane, we have found that knockout of TMEM16F from microglia additionally results in increased release of exosomes, extracellular vesicles derived from exocytosis of multivesicular bodies. Microglial exosomes have been implicated in the spread of soluble tau oligomers in the P301S mouse model of tauopathy. We sought to investigate the pathological effect of increased microglial exosomes from TMEM16F knockout in these tauopathy mice. When TMEM16F was removed from microglia, we observed worsening of hyperphosphorylated tau and microgliosis, suggesting an increase in exosomes can contribute towards pathology. However, when TMEM16F was knocked out from all cells, we found the opposite phenotype, with knockout mice having a reduction in pathology compared to those with TMEM16F intact. In P301S mice, neurons have been shown to aberrantly expose phosphatidylserine (PS), targeting them for premature death by microglia. Thus, we investigated if neurons with pathological tau burden and removal of TMEM16F still experienced this PS exposure and whether a deficiency in PS exposure may explain the reduction in pathology. *In vitro* cultures of tau burdened TMEM16F knockout neurons exposed less PS and had fewer interactions with WT microglia that were added to the neuronal cultures. These findings suggest TMEM16F may become activated in neurons with tauopathy to expose PS while TMEM16F in microglia may influence the balance of microvesicle and exosome release. Better understanding of TMEM16F may facilitate its manipulation in various cell types toward future development of therapeutics.

# Table of Contents

<b>CHAPTER 1: INTRODUCTION .....</b>	<b>1</b>
1.1 TMEM16F and the TMEM16 Family .....	2
1.1.i Founding members of the TMEM16 family .....	2
1.1.ii TMEM16 family members have broad functions throughout the body.....	3
1.1.iii Scott syndrome and TMEM16F as a lipid scramblase .....	3
1.1.iv Insights of lipid scrambling by comparison of TMEM16A and TMEM16F.....	5
1.1.v Diverse roles of TMEM16F and its ability to scramble lipids .....	5
1.2 Extracellular Vesicles.....	6
1.2.i Classes and origins.....	6
1.2.ii Extracellular vesicles in physiology throughout the body and the brain.....	7
1.2.iii Extracellular vesicles in disease .....	8
1.3 Neurodegeneration and tauopathy.....	9
1.3.i The brain and neurodegenerative disorders .....	9
1.3.ii Alzheimer’s disease and tauopathies .....	9
1.3.iii Tau and NFTs.....	10
1.2 FIGURES .....	12
<b>CHAPTER 2: Functional roles of TMEM16F in microglia.....</b>	<b>13</b>
2.1 INTRODUCTION .....	14
2.2 RESULTS.....	15
2.2.i TMEM16F is enriched in all extracellular vesicles .....	15
2.2.ii TMEM16F KO microglia secrete fewer microvesicles and more exosomes.....	16
2.2.iii TMEM16F KO increases cell size in BV2, but not primary microglial cells .....	16
2.2.iv TMEM16F KO microglia have enhanced phagocytic ability .....	17
2.3 DISCUSSION .....	18

2.4 FIGURES .....	22
<b>CHAPTER 3: TMEM16F mediates aberrant neuronal lipid scrambling in the P301S</b>	
<b>model of tauopathy .....</b>	<b>25</b>
3.1 INTRODUCTION .....	26
3.2 RESULTS.....	27
3.2.i <i>Conditional microglial knockout of TMEM16F in PS19 mice worsens disease progression.....</i>	<i>27</i>
3.2.ii <i>PS19+ conditional TME1M16F KO mice have partially perturbed behavior .....</i>	<i>28</i>
3.2.iii <i>Tau pathology is exacerbated in PS19 conditional TMEM16F KO mice.....</i>	<i>29</i>
3.2.iv <i>Global knockout of TMEM16F reduces disease progression in PS19 mice .....</i>	<i>29</i>
3.2.v <i>TMEM16F KO reduces PS exposure from tau burdened neurons .....</i>	<i>30</i>
3.2 vi <i>Microglia have fewer interactions with tau burdened TMEM16F KO neurons .....</i>	<i>31</i>
3.4 DISCUSSION .....	31
3.5 FIGURES .....	36
<b>CHAPTER 4: CONCLUDING REMARKS.....</b>	<b>44</b>
4.1 CONTRIBUTIONS TO THE FIELD.....	45
4.2 FUTURE DIRECTIONS .....	46
4.2.i <i>Mechanistic insights into TMEM16F and extracellular vesiculation.....</i>	<i>46</i>
4.2.ii <i>Targeted TMEM16F manipulation may prove therapeutic in tauopathy .....</i>	<i>47</i>
<b>CHAPTER 5: MATERIALS AND METHODS.....</b>	<b>49</b>
5.1 FIGURES .....	61
<b>REFERENCES .....</b>	<b>62</b>

## LIST OF FIGURES

Figure 1.1. Extracellular vesicles and the endolysosomal pathway.....	12
Figure 2.1. Knockout of TMEM16F from microglia alters extracellular vesiculation. ....	22
Figure 2.2 BV2 TMEM16F KO cells are larger than WT, while primary cells exhibit no differences in size.....	23
Figure 2.3 TMEM16F KO cells have enhanced phagocytosis and acidification. ....	24
Figure 3.1 7-month-old, but not 6-month-old PS19 Cx3cr1-Cre mice display differences in disease pathology.....	36
Figure 3.2 Baseline activity and anxiety slightly perturbed. ....	38
Figure 3.3 Modest impairment to visual/ spatial learning in PS19+ conditional TMEM16F KO mice.....	39
Figure 3.4 TMEM16F KO in microglia worsens pathology in tauopathy. ....	40
Figure 3.5 Complete TMEM16F knockout reduces progression of disease.....	41
Figure 3.6 TMEM16F KO reduces PS exposure in P301S neurons.....	42
Figure 3.7 Microglia have fewer interactions with AT8+ TMEM16F KO neurons.....	43
Figure 5.1 Schematic of extracellular vesicle collection.....	61

**LIST OF TABLES**

**Table 5.1. CRISPR/ Cas9 sgRNA guides.....50**

## **CHAPTER 1: INTRODUCTION**



## 1.1 TMEM16F and the TMEM16 Family

Mammalian transmembrane protein 16F (TMEM16F), also known as anoctomin-6 (Ano6), is a calcium-activated phospholipid scramblase and small-conductance ion channel. While the TMEM16F gene was first identified in 2004 [1], its function as a lipid scramblase was not discovered until 2010 [2]. In the decade since, researchers have begun to understand the diverse roles TMEM16F plays throughout the body and have utilized its properties as a lipid scramblase to probe mechanistic studies of how lipids can move across the bilayer and how this may lead to downstream cellular processes, including extracellular vesiculation [3-8].

### 1.1.i Founding members of the TMEM16 family

TMEM16F is a member of the TMEM16 family of  $\text{Ca}^{2+}$ -activated ion channels and lipid scramblases (A-K, excluding I) that have a wide milieu of functions and roles throughout the body [5, 6, 8]. For decades, scientists knew of the importance of calcium-activated chloride currents in a variety of physiological functions but had been unsuccessful in identifying its source [9]. In 2008, three independent research groups—including the Jan laboratory—identified unambiguously, using different techniques and expression systems, that TMEM16A and its close paralog TMEM16B (82% transmembrane domain sequence similarity) were responsible for this current [10-12].

These two founding members, TMEM16A and TMEM16B have been well studied since their identification and are well established as  $\text{Ca}^{2+}$ -activated chloride channels. Their channel activity plays roles in control of neuronal excitability, transepithelial ion transport, primary ciliogenesis, olfaction, phototransduction, smooth muscle contraction, nociception, and cell proliferation [5, 6, 8, 13]. When misregulated, they have implications in disease, such as TMEM16A overexpression correlated with prognosis in many cancers or TMEM16B being an autoimmune target in multiple sclerosis [14, 15]. In addition to TMEM16A and TMEM16B, calcium-activated chloride channel activity has also been found in the *Drosophila* homolog,

Subdued [16]. This current, however, has not been definitively shown from any other family members. While TMEM16E, TMEM16F, and the fungal homologs nhTMEM16 and afTMEM16 have possible dual function as a channels and phospholipid scramblases, most other TMEM16 members are either only phospholipid scramblases or still have unknown function [17-19].

#### *1.1.ii TMEM16 family members have broad functions throughout the body*

The TMEM16 family has expression across the entire body and may serve a variety of functions in many cellular processes and tissues. TMEM16A is expressed in all secretory epithelium, certain smooth muscles, and sensory neurons [5, 8, 10]. TMEM16B is found in central neurons and controls neuronal excitability in multiple brain regions including hippocampus, inferior olive, thalamus, retina, and lateral septum [20, 21]. TMEM16C is expressed in the central nervous system (CNS) and has been implicated in febrile seizures and sensory neuronal pain processing [5, 8, 22]. Studies of TMEM16E have linked it to multiple musculoskeletal disorders including several muscular dystrophies, myopathies, and skeletal dysplasias [23-25]. It is localized predominantly to intracellular membrane vesicles and plays a role in membrane repair [6, 23-25]. TMEM16F has low expression throughout almost all cells in the body, including all immune cells probed thus far, and has an important role as a phospholipid scramblase [2, 26-29]. TMEM16G is highly expressed in the prostate and has expression very similar to that of prostate cancer genes [30]. TMEM16K expression is found in the CNS and in numerous immune cells. It is an interorganelle regulator of endosomal sorting and its mutation leads to spinocerebellar ataxia [31]. Other TMEM16 members have unknown function, but research into the entire family is rapidly expanding.

#### *1.1.iii Scott syndrome and TMEM16F as a lipid scramblase*

As stated previously, only TMEM16A and TMEM16B have been shown to be bona fide  $\text{Ca}^{2+}$ -activated chloride channels. Instead, most other members including TMEM16C,

TMEM16D, TMEM16E, TMEM16F, TMEM16G, and TMEM16K have been shown to have phospholipid scrambling ability [32, 33].

Mammalian cell membranes are composed of a phospholipid bilayer with asymmetrically distributed lipids including phosphatidylserine (PS), phosphatidylethanolamine (PE), and phosphatidylinositols (PIs) on the inner leaflet and phosphatidylcholine (PC) and various glycosphingolipids (including sphingomyelin (SM) and gangliosides) on the outer leaflet [34-36]. This process is established and maintained through ATP-dependent unidirectional phospholipid translocases that can either bring aminophospholipids from the outer leaflet inward towards the cytoplasm (P4-ATPases) or oppositely, move other lipids from the inner leaflet to the luminal side (ATP-binding cassette (ABC) transporters)—referred to as “flippases” and “floppases,” respectively [36-38]. Phospholipid scramblases are a third class of proteins that can reversibly move these lipids bidirectionally from one leaflet to the other in a calcium-dependent, energy-independent manner. This leads to transient or sustained collapse of membrane asymmetry, similar to the case of apoptotic scrambling [37, 38].

Patients with a rare bleeding disorder called Scott syndrome have a deficit in coagulation, which is attributed to platelets deficient in lipid scrambling [39]. During coagulation, anionic lipids on platelets promote assembly of factors and accelerate formation of thrombin, which allows a blood clot to form quickly [39]. Exposure of these negatively charged lipids, which are normally sequestered on the inner leaflet, is crucial to this cascade [39]. While phospholipid scramblase 1 (PLSCR1) was initially thought to be the scramblase involved in Scott syndrome [40, 41], its knockouts in mice and *Drosophila* ruled it out to be a scramblase completely [42]. It was discovered that Scott syndrome patients have mutations that lead to truncation of TMEM16F mRNA [2, 43]. Scott syndrome patient cells bearing these mutations were confirmed to have calcium-activated scrambling deficits [2] and TMEM16F knockout mice additionally had both deficiencies in scrambling and blood coagulation [7]. This identification of

TMEM16F as an elusive scramblase has launched much research into the cellular dynamics of lipid asymmetry and consequence of collapse of plasma membrane asymmetry.

#### *1.1.iv Insights of lipid scrambling by comparison of TMEM16A and TMEM16F*

There is much interest in understanding the varied function of TMEM16 family members. All TMEM16 proteins have 10 transmembrane domains and can form homodimers, with each monomer coordinating two  $\text{Ca}^{2+}$  ions [44-46]. Analysis of different TMEM16 members has identified those members that are able to scramble (TMEM16C, -D, -E, -F, -G, -K) and particular domains which impart scrambling ability [32, 47, 48]. Cryo-EM structures of TMEM16 fungal homologues, TMEM16A, and TMEM16F have also revealed a possible pathway for lipid scrambling along a hydrophilic groove separate from an ion permeation channel [45, 49-52]. Better understanding of how lipids are scrambled will allow for development of pharmacological modulators of scrambling activity and its downstream effects.

#### *1.1.v Diverse roles of TMEM16F and its ability to scramble lipids*

A direct consequence of lipid scrambling from platelets is release of microvesicles that aid in coagulation [27]. Apart from coagulation, TMEM16F has been identified to have many other roles throughout the body. Initial assessment of B and T cells from Scott syndrome patient cells show scrambling deficits [2] and a later studies identified TMEM16F as mediating secretion of sheddase ADAM10, which is often dysregulated in tumorigenesis and some neurodegenerative disorders, from these cells [53]. TMEM16F on T cells has been shown to be important for regulation of T cell receptor secretion at the immunological synapse to prevent exhaustion during infection [54]. It has also been shown to be important for T cell membrane expansion and release of PD-1, which is a negative regulator of inflammation [26]. Researchers have demonstrated that HIV-1 fusion depends upon activation of TMEM16F; PS aids in HIV-1 envelope binding on target T cells [55]. Furthermore, in infected cells of HIV-1 or Ebola virus, replication of virus and release of virions is dependent upon PS exposure mediated by

TMEM16F [56, 57]. TMEM16F also has roles in membrane repair after pore formation [58]. In arthritis, TMEM16F in neutrophils allows for the formation of microvesicles containing Annexin A1 to provide resolution to inflammation within the synovium [59]. During bone formation, TMEM16F is important for osteoblast matrix vesicle formation [60]. Additionally, a few studies have examined TMEM16F's role in the nervous system. TMEM16F is important in recruitment of fast  $\alpha$ -motor neurons to C-boutons of motor neurons [61], in microglial (dys)function in neuropathic pain states [62] and in polarization following spinal cord injury [63], and most recently, in exposure of PS in neurons after cerebral ischemia [64]. Importantly, many of these identified roles of TMEM16F in lipid scrambling lead to extracellular vesiculation and that it is these vesicles that impart effect on other cells or processes.

## *1.2 Extracellular Vesicles*

Very little is known about the role of extracellular vesicles (EVs) in physiology and disease. Extracellular vesicles are membrane-enclosed bodies of various origins and sizes that are released into the extracellular space and are able to transport lipids, proteins, and various RNA species [65-70].

### *1.2.i Classes and origins*

Extracellular vesicles consist of three main populations: apoptotic bodies, microvesicles (MVs), and exosomes. Apoptotic bodies (1-5  $\mu\text{m}$ ) are cellular blebs released during apoptosis [71]. Microvesicles (100 nm-1  $\mu\text{m}$ ), also known as microparticles or ectosomes, are EVs secreted by direct outward budding from the plasma membrane (**Figure 1.1**) [71]. Exosomes (30-100 nm), the smallest EVs, are intraluminal vesicles (ILVs) that are released through exocytosis of multivesicular bodies (MVBs) (**Figure 1.1**) [72, 73]. ILVs are formed by reverse budding into the lumen of late endosomes and are released as exosomes when MVBs fuse to the plasma membrane [72, 73]. It is important to note that while size proves useful in attempts

to distinguish extremes of these different species of EVs, there is a large heterogeneity amongst different populations and overlap exists [67].

Identifying universal markers for different populations has been a long sought-after goal in the extracellular vesicle field. However, as with size heterogeneity, many EVs of the same type have different markers depending on cell of origin or physiological state [72]. Because of the main ways in which they are processed and formed, markers on exosomes often contain various proteins enriched in endosomes or endosomal membranes, such as tetraspanins (CD9, CD63, CD81, CD82), heat shock proteins, MHC complexes, TSG101, or members of the ESCRT machinery, involved in sorting and scission of ILVs into endosome, which form MVBs [67]. Endosomal sorting complex required for transport (ESCRT) proteins involved in biogenesis of ILVs and MVBs consist of about 20 proteins that form four complexes (ESCRT-0, -I, -II, -III) and associate with VPS4, VTA1, and Alix [74, 75]. ESCRT-0 recognizes and brings ubiquitinated proteins to endosomes, ESCRT-I and -II help with membrane deformation and budding, and ESCRT-III helps with scission [76, 77]. Microvesicles also, however, utilize ESCRT for scission, so many of the proteins initially thought to be exosome specific are also found on MVs [78]. Some MVs utilize the small GTPase ADP-ribosylation factor 6 (ARF6), as it recruits some proteins to the plasma membrane including  $\beta$ 1 integrins, MHC class 1 molecules, membrane type 1-matrix metalloproteinase (MMP14), and VAMP3. Many studies will use size and show exclusion on TSG101 or HSP70 to characterize a microvesicle population. As stated, however, different cells modulate their machinery depending on its function and even within one cell type, multiple forms of exosomes or MVs and cargoes can exist [78].

#### *1.2.ii Extracellular vesicles in physiology throughout the body and the brain*

Extracellular vesicles have been shown to have many roles throughout the body, especially for cellular communication. The cargoes of EVs can contain proteins, messenger RNAs (mRNAs), micro RNAs (miRNAs), and DNA [72, 79]. Effects of these cargoes on recipient

cells are broad and can help maintain cell homeostasis [80], affect cell survival [81], induce cellular signaling after either binding or release of content [71, 82, 83], altering gene expression [84], or help protect or repair tissue [85]. While most studies involve the periphery, research into EVs and the nervous system has also been rapidly expanding [86]. Gene expression is altered in astrocytes upon uptake of neuronal exosomes containing miR-124a, leading to upregulation of excitatory amino acid transporter 2 (EAAT2), an important mediator of glutamate uptake in the brain [87]. Oligodendrocyte EVs have been shown to secrete exosomes with proteolipid protein (PLP), myelin proteins, and proteins against oxidative stress, and can be released upon glutamate release from neurons [88, 89]. They have also been shown to release EVs which inhibit myelination and differentiation through absence of neurons [90]. Microglial MVs have been shown to modulate neuronal excitability [91, 92]. Their exosomes can have similar content to peripheral immune cells under basal condition (MHCII, chaperones, tetraspanins, CD13) [93] and release may be influenced by neurotransmitters, including serotonin [94]. In response to binding of P<sub>2</sub>X<sub>7</sub> receptors, both microglia and astrocytes can release MVs with IL-1 $\beta$  [95, 96], and astrocyte EVs have been shown to contain synapsin 1 [97].

### *1.2.iii Extracellular vesicles in disease*

Exosomes and MVs have been implicated in several disorders, including cardiovascular disease, thrombosis, arthritis, and cancer metastasis [69, 98-102]. The surge in EV research was, in part, mediated by studying cancer cells and exploring tumor EVs and their effect on metastasis and either up or downregulation in target cells [78, 98]. Recent studies have explored the role of exosomes in neurodegeneration. Researchers have demonstrated that exosomes are able to spread toxic forms of aggregate-prone proteins such as alpha synuclein in Parkinson's disease, amyloid beta in Alzheimer's disease, and tau in tauopathies [103-107]. In particular, EVs from microglia, immune cells of the brain, have been shown to contain proinflammatory cytokines as well as these toxic forms of proteins [96, 103, 107, 108].

## **1.3 Neurodegeneration and tauopathy**

### *1.3.i The brain and neurodegenerative disorders*

The brain is the most complex organ in the body. Its nearly 100 billion neurons help to connect, orchestrate, and sync system function throughout the body through about 100 trillion synapses [109]. While neurons relay the electrical and chemical signals throughout the body, there are numerous other cell types pivotal to brain function such as microglia, astrocytes, oligodendrocytes, and NG2-glia [110].

Neurodegenerative disease is characterized by the progressive degeneration of neurons, either in their structure and connectivity or in their function, leading to cell death. There are many types of neurodegenerative disorders including, but not limited to, Alzheimer's disease (AD), frontotemporal dementia (FTD) and its variants, progressive supranuclear palsy (PSP), Parkinson's disease, corticobasal degeneration (CBD), dementia with Lewy bodies, multiple system atrophy, multiple sclerosis, lateral amyloid sclerosis, and Huntington's disease [111]. Alzheimer's disease alone affects 24 million people worldwide [111]. These disorders have a broad range of clinical syndromes and underlying pathologies, but many share a common pathological hallmark of a protein exhibiting prion-like behavior, damaging the neuron it is within, and upon spreading causing healthy neurons to become diseased [111]. Clinical syndromes that manifest are often a result of the particular subset of neurons that are affected and what their normal physiological role is [111]. Unlike most other cells in the body, neurons do not undergo cell division, enhancing the need to develop therapeutics to prevent this irreplaceable loss from neurodegeneration.

### *1.3.ii Alzheimer's disease and tauopathies*

Alzheimer's disease is the most common form of dementia, accounting for 60 to 80% of all cases and affecting 24 million people worldwide and 5 million Americans [109, 111]. In the United States, it is the sixth leading cause of death and fifth in people 65 or older, with over



122,000 deaths in 2018 alone [109]. Care for patients in 2020 was valued at \$305 billion and an estimated \$244 additional unpaid care from more than 16 million family members [109]. As the population ages, AD presents a huge societal health crisis that must be tackled.

Alzheimer's disease is characterized by the buildup of extracellular amyloid beta ( $A\beta$ ) plaques and intracellular neurofibrillary tau tangles (NFTs), including smaller oligomers of both which also impede neuronal function [112, 113]. In addition to pathology caused by these two proteins, AD is accompanied by inflammation and brain atrophy [111, 114]. Amyloid beta is thought to form plaques prior to tau tangle formation and for many years it was thought to have more weight in disease progression [109]. However, both have been shown to induce deficits and degeneration, and furthermore, the rate of tau, rather than  $A\beta$ , changes is associated with cognitive deficits [113]. Additionally, clinical trials for Alzheimer's targeting  $A\beta$  have failed in late stage, raising the question whether tau therapeutics may be more promising [115].

While AD is the most common dementia, neurofibrillary tangles are the most common intracellular inclusion and are found in most neurodegenerative disorders; over twenty-five are classified as tauopathies [116]. Tau deposits are the predominant pathological signature in PSP, CBD, frontotemporal dementia and parkinsonism linked to chromosome 17 (FTDP-17), Pick's disease (PiD), chronic traumatic encephalopathy (CTE), and argyrophilic grain disease (AGD). Because many mechanisms are shared across these diseases, it can be beneficial to study tauopathies as a whole.

### *1.3.iii Tau and NFTs*

Tau is a 45 to 65 kDa microtubule-associated protein (MAP) important for microtubule scaffolding throughout the cell and along axons [116]. Tau proteins are made up of four distinct domains, with their N terminal projection domains and microtubule-binding repeat domains (MTBD) varying in number resulting in 6 different splice isoforms that have various spatial and temporal distribution throughout the brain [117]. The N terminal domain is made of either one

(1N) or two repeats (2N) and is important for spacing between microtubules and axon diameter [116, 117]. The MTBD is made of three (3R) or four (4R) highly conserved repeat motifs that can bind microtubules through an array of weak sites [118]. Tau is an intrinsically disordered protein meaning it has no stable sequence-defined secondary structure. This allows for easier access to phosphorylation, among other modifications, and can decrease its affinity to microtubules, which in healthy neurons, ensures dynamics [119, 120]. However, in tauopathies, mutations lead to hyperphosphorylation, and dissociation of tau from microtubules eventually leads to their formation of NFTs in the cytosol [116, 120]. Various species of NFTs or oligomers of tau fibrils exhibit prion-like behavior, where there is a generation of a tau fibril seed that can be secreted from burdened neurons, taken up by an unaffected cell, and then serve as a template for more misfolded tau [120, 121].

## 1.2 FIGURES

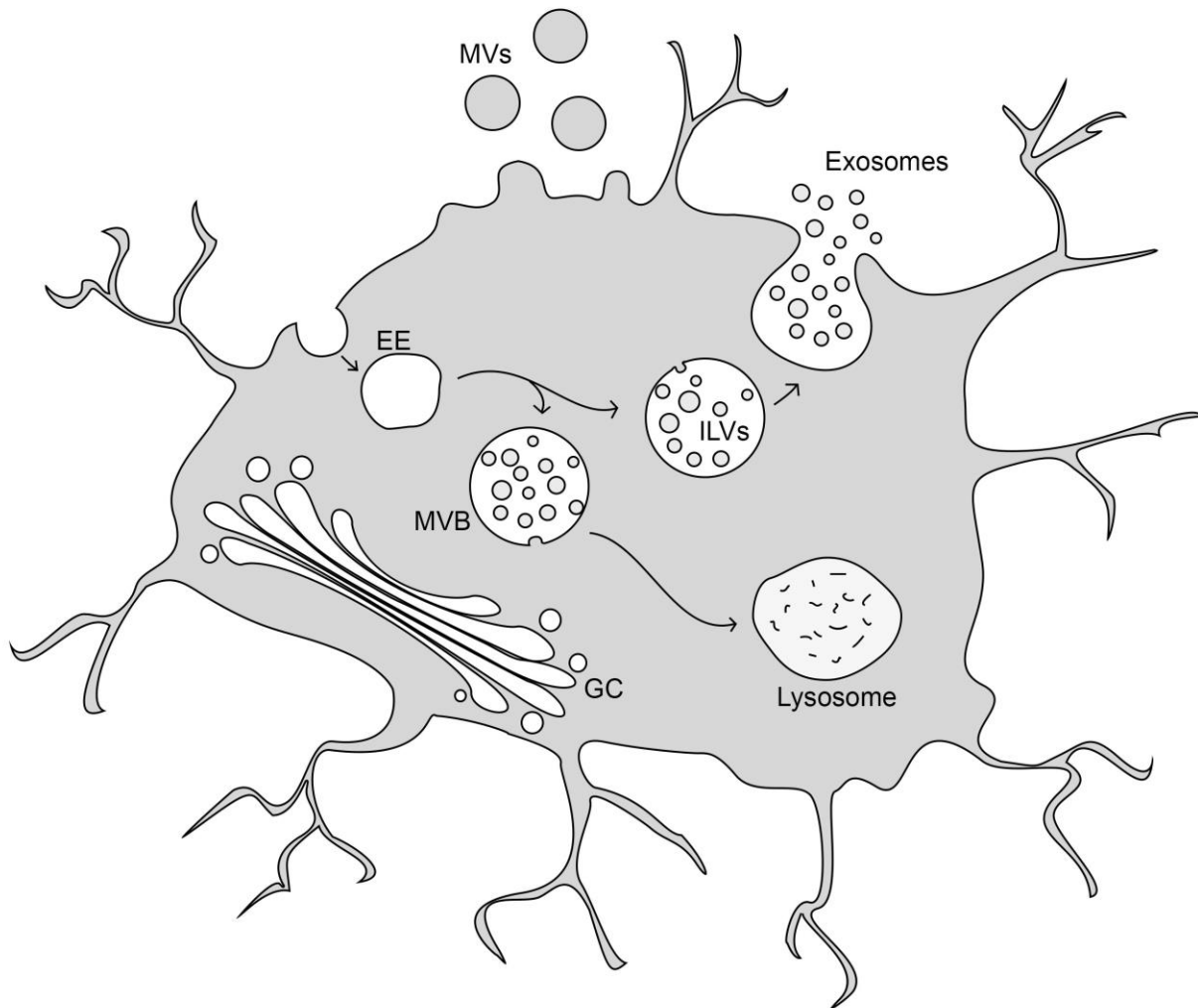


**Figure 1.1. Extracellular vesicles and the endolysosomal pathway.** Apart from apoptotic bodies (1 - 5  $\mu\text{m}$ ) that bleb from the cell during apoptosis, two other extracellular vesicles are microvesicles (MVs)(100 nm - 1  $\mu\text{m}$ ) and exosomes (20 – 150 nm). After endocytosis, early endosomes (EEs) mature into late endosomes/ multivesicular bodies (MVBs), containing inwardly-budded intraluminal vesicles (ILVs). MVBs can be targeted for the lysosome, where ILVs are degraded or brought to the plasma membrane, where ILVs are released as exosomes. Abbreviations: EE = early endosome, MVs = microvesicles, MVB = multivesicular body, ILVs = intraluminal vesicles, GC = Golgi complex.

## **CHAPTER 2: Functional roles of TMEM16F in microglia**

## 2.1 INTRODUCTION

Microglia are the resident immune cells of the brain. Throughout development and aging, they help to prune synapses, scavenge, clear apoptotic debris, and are the first line of defense against brain pathologies or assault [122-126]. Unlike other organs in the body, the brain is protected by a semipermeable seal—the blood brain barrier—which under normal physiology does not allow for entry by other cells, including those of the immune system. Because of this, microglia's roles are vast. But likewise, because they play many pivotal roles, dysregulation often manifests alongside neurodegenerative disorders, where improper clearance of pathological protein aggregates or hyperinflammation due to these aggregates further damage neurons [127].

Yolk sac progenitor cells enter the neural tube during embryonic development at E9.5 and are the only such brain cell not derived from neuroectoderm [128]. Other tissue resident macrophages, similarly enter their respective tissues as yolk sac progenitors and persist through self-renewal instead of through bone marrow-derived monocytes that become macrophages in circulation [128]. However, because these cells share common lineage, they also share many of the same molecular signatures [125, 127, 129] and thus functions and abilities including phagocytosis of apoptotic cells or pathogens [130], surveillance [131], and secretion of pro- and anti-inflammatory cytokines and chemokines [125].

Brain specific function of microglia begin early in development with aiding in differentiation [132] and migration of neurons and other glia such as astrocytes [133], promoting formation of synapses [134], as well as synapse removal with aide of the complement proteins [123]. In the adult, microglia can modulate neuronal activity [135], promote neurogenesis [136], and like in development, prune synapses, which in adulthood can affect memory and learning [137]. In pathology, microglia are important for phagocytosis and inducing inflammation for clearance of aggregate proteins and dying cells and have unique disease associated microglia (DAM) signatures [127, 138]. Large genome wide association studies (GWAS) have identified

risk factors and single nucleotide polymorphisms (SNPs) in genes that encode microglial proteins that have function in these processes, including TREM2, CD33, and APOE found in DAM [139]. While production of inflammatory cytokines and chemokines aid in clearance, microglia often become overwhelmed and can lose proper ability of sensing, housekeeping, and host-defense and thus an inflammatory state and now improper clearance worsens progression of disease [127, 138, 140]. Taken together, it is evident that the role of microglia in neurodegeneration is a double-edged sword and understanding the balance of neuroinflammation continues to be an important to understanding disease pathogenesis [127, 140].

TMEM16F had been studied or its expression found in various immune cells including platelets, erythrocytes, T cells, B cells, neutrophils, and macrophages [2, 3, 7, 27, 54, 59]. We thus sought to examine the role it may have in microglia, which as previously mentioned, has many cellular functions found in these immune cell counterparts.

## **2.2 RESULTS**

### *2.2.i TMEM16F is enriched in all extracellular vesicles*

TMEM16F's role in regulation of microvesicles (MVs) was well known from previous studies in other immune cells [3, 7, 59], so we wanted to confirm this phenotype in microglia. Microglia utilize vesicles for extracellular communication and various forms of x, y, z.

We first knocked out TMEM16F from the microglial BV2 cell line using CRISPR-Cas9 technology with guides against exon 2 (described in **Ch4: Materials and Methods, Table 4.1**), which resulted in a premature stop codon in a similar location to that of the mutation found in Scott Syndrome [43]. To collect microvesicles and other extracellular vesicles (EVs), we stimulated cells with a pulse of calcium ionophore A23187 and then collected media after 90 minutes of incubation. Collected supernatant was spun down through differential ultracentrifugation to isolate different EVs which either pellet or remain in suspension depending

on the speed of centrifugation (**Ch4: Materials and Methods, Figure 4.1**). An important caveat, however, is that differential ultracentrifugation does not fully distinguish exosomes from MVs, but instead gives a rough estimate of different populations based on size. When different extracellular vesicle populations were probed for TMEM16F expression via Western blot, we saw enrichment of TMEM16F not only in MVs, which is known from previous studies, but also in exosomes (**Figure 2.1A**). We confirmed that our samples were positive for Alix, an ESCRT-associated protein and saw that upon  $\text{Ca}^{2+}$  stimulation, its expression increased (**Figure 2.1B**).

#### *2.2.ii TMEM16F KO microglia secrete fewer microvesicles and more exosomes*

Different EV populations were quantified using Nanosight nanoparticle tracking analysis (NTA), that uses Brownian motion to determine particle size and ImageStream<sup>X</sup> flow cytometry, which in addition to fluorescence, forward scatter (FSC) and side scatter (SSC), also uses microscopy to take an image of each event. While NTA is better suited for smaller EVs like exosomes, ImageStream<sup>X</sup> flow cytometry can better quantify MVs [141]. After  $\text{Ca}^{2+}$  stimulation with calcium ionophore A23187, TMEM16F KO BV2 cells release fewer MVs compared to WT, as has been shown for numerous other cell types (**Figure 2.1C**). Despite releasing fewer MVs, they also surprisingly, secrete more exosomes (**Figure 2.1C**). We verified these results using three independent knockout BV2 cell lines, suggesting this phenotype was not due to an off-target effect of the CRISPR/ Cas9 sgRNAs. When primary microglia were cultured and extracellular vesicles were collected and counted, we observed the same increase in exosomes from TMEM16F KO cells (**Figures 2.1D**).

#### *2.2.iii TMEM16F KO increases cell size in BV2, but not primary microglial cells*

To begin to explore possible mechanisms behind this increase, we quantified cell size between genotypes. During culture of WT and TMEM16F KO BV2 cells, we observed that knockout cells appeared larger than WT. TMEM16F has been suggested to regulate volume [142]. It is possible that larger cells have more membrane available or have more volume within

the cytoplasm for multivesicular bodies and thus may result in more exosomes being released. In BV2 cells, we found that TMEM16F KO cells segregated from WT, both with FSC and SCC, with these KO cells thus being larger and more granular, respectively (**Figure 2.2A-B**). BV2 cultures that were imaged with brightfield microscopy also showed that knockout cells were larger than wildtype (**Figure 2.2C-D**). To see if this volume increase applies to primary microglia, which also secrete more exosomes in the absence of TMEM16F, we analyzed primary cells. Flow cytometric analysis showed KO cells were the same size as WT (**Figure 2.2 E-F**). This was confirmed by brightfield microscopy (**Figure 2.2G**). This suggests that while larger cell size may partly contribute to more exosome secretion in BV2 cells, this alone, does not explain increased exosome release, as this cell size difference is not present in primary microglia.

#### *2.2.iv TMEM16F KO microglia have enhanced phagocytic ability*

Another possible explanation for increased exosome release may be deficient degradation of intraluminal vesicles (ILVs) within late endosomes. In the endolysosomal pathway, only a few multivesicular bodies (MVBs) fuse with the plasma membrane to release exosomes. The remainder will fuse with lysosomes leading to the degradation of ILVs [72, 83]. In macrophages infected with mycobacteria, where exosome secretion is increased, MVBs and phagosomes are nonfusogenic with lysosomes and fail to acidify [143, 144]. In SH-SY5Y neuronal-like cells overexpressing alpha synuclein, impairment of lysosomal function results in increased exosomes containing alpha synuclein. Recently, it was also shown that knockdown of NDRG1, a cytoplasmic protein involved in regulation of endosome trafficking, or use of pharmacologic inhibitors of endolysosomal trafficking—chloroquine or  $\text{NH}_4\text{Cl}$ —all resulted in increased exosome release [145]. In all cases, impaired lysosomes or impaired trafficking to the lysosome leads to inadequate degradation of ILVs from MVBs or phagosomes, leading to their



release upon MVB fusion to the plasma membrane. In TMEM16F KO cells, it is possible that insufficient degradation is a cause for the release of more ILVs.

To first probe whether general lysosome machinery or trafficking to the lysosome was impaired, we decided to look at phagocytosis, a cellular process by which microglia rely heavily on their lysosomes for degradation of phagocytosed material. We assayed phagocytosis using pH sensitive fluorophore-conjugated *E. coli* particles (pHrodo *E. coli*) that fluoresce upon reaching the lysosome. We found that TMEM16F KO cells have increased acidification of *E. coli* particles, as a metric of phagocytic ability, compared to WT (**Figure 2.3A**). We also observed this increase in acidification when we performed this assay in primary microglia with TMEM16F knocked out (**Figure 2.3B**). To ensure acidification was not due to increased cell death, which results in alteration of cellular pH [146], we also utilized live imaging microscopy to visualize pHrodo *E. coli* particles (**Figure 2.3C**). Additionally, we used Alexa 594-conjugated *E. coli* and measured signal within microglia at various timepoints (data not shown). Knockout cells phagocytosed more *E. coli* and the signal was punctate, perinuclear and not broadly cytoplasmic suggesting there was not increased cell death from these cells (**Figure 2.3C-D**). While phagocytosis is one of many processes by which early endosomes may form, the lack of impairment and furthermore increased ability does not suggest that lysosome machinery is contributing to increased exosome release.

## 2.3 DISCUSSION

The discovery of TMEM16F as a lipid scramblase has introduced many new approaches to study cellular processes that rely upon lipid asymmetry—one of which is extracellular vesiculation [38, 83, 147, 148]. TMEM16F was first identified to be responsible for both PS exposure on platelets in coagulation and also release of platelet microvesicles [27]. All studies examining TMEM16F thus far have focused on microvesicles, but our data provide the first

evidence of its effect on exosomes. We found that knockout of TMEM16F from microglia both reduces the release of MVs and increases the secretion of exosomes.

Although the mechanism behind TMEM16F mediated MV biogenesis is not fully known, it is proposed that lipid scrambling may both destabilize the plasma membrane and create a local lipid profile conducive toward recruitment of factors to help with budding and scission [83, 148, 149]. Increased exosome release from TMEM16F knockout cells after  $\text{Ca}^{2+}$  stimulation likely involves disruption of the phospholipid bilayer, but it is important to first identify where in exosome biogenesis and release TMEM16F is playing a role. Exosomes originate from the exocytosis of ILVs when MVBs fuse to the plasma membrane [72, 83]. ILVs form from the maturation of endosomes through the endolysosomal pathway, so there are several locations in which TMEM16F may be acting.

In TMEM16F KO, one possible change may be differences in MVBs under basal conditions. An increase in the number of MVBs produced or an increase in the number of ILVs within each MVB could result in more exosomes being released. Furthermore, because TMEM16F can scramble lipids and phospholipid composition is essential to membrane curvature of inward budding of ILVs, it is conceivable that dysregulation of scrambling may lead to more ILVs or MVBs being produced. Lipid domains have been implicated in protein targeting for docking and fusion of MVBs to the plasma membrane [150-152]. Additionally, membrane curvature important for inward budding of ILVs may depend on lipid composition of the MVB membrane [153, 154]. Late endosomes are highly enriched in sphingolipids and cholesterol [154, 155]. On endosomes, which have sphingolipids on their inner leaflet, movement of sphingomyelin (SM), a particular sphingolipid, to the outer membrane, allows for neutral sphingomyelinase 2 (nSMase2) to convert SM into ceramide [154, 156, 157]. Ceramide, which contains monosaturated fatty acid chains, is able to cluster together with a much higher propensity than other polysaturated lipids, and cholesterol further stabilizes ceramide into lipid rafts [154, 156]. Ceramide lipid rafts promote negative curvature, which allows for inward

budding of ILVs from these late endosomes, thereby forming MVBs [154, 156]. If in TMEM16F KO cells, there are increased ILVs within MVBs, WT TMEM16F may be responsible for maintaining balance of SM on the inner leaflet.

It is important to note, in the Jurkat T cell line, Hu and colleagues found that knockdown of TMEM16F results in no difference at basal state, but a reduction of ILVs after T cell receptor (TCR) stimulation [54]. They hypothesize this reduction in ILVs results in deficits in resolving TCR activation, as fewer activated TCRs would be sorted for degradation. They also show that knockout T cells exhibit higher levels of PD-1 and are less effective late into chronic infection [54]. Later studies by Bricogne and colleagues showed that TMEM16F instead traffics PD-1 and that its downregulation is through this mechanism of release in extracellular vesicles [26]. These differences suggest different activation of T cells may result in various EV biogenesis pathways and that in microglia after Ca<sup>2+</sup> stimulation, there still may be increased ILVs in TMEM16F knockout cells.

We showed that there was not a deficit and instead an enhancement of acidification of *E. coli* particles after phagocytosis by TMEM16F KO cells. It is still possible, however, that increased number of MVBs through mechanism of improper degradation or targeting can lead to increased exosome secretion. For microglia, *E. coli* is a non-physiologic antigen that it would not normally encounter. Future studies should examine fluorescently labeled apoptotic cells or debris or utilize another type of degradation along the endolysosomal pathway, such as EGF/EGFR [158, 159]. Upon binding to its receptor, EGF can be tracked along early to late endosomes and ultimately to the lysosome[158].

Regarding phagocytosis, Batti et al. and Zhao et al. found that TMEM16F knockout impairs phagocytic and inflammatory ability of spinal microglia [62, 63]. Batti and colleagues knocked out TMEM16F from monocytic lineage marker LysM, while Zhao and colleagues used a complete knockout mouse line [62, 63]. In the complete knockout, microglia had fewer pro-inflammatory markers [63]. The authors suggest this is due to impairment of inflammatory

ability. However, an additional interpretation may be that neurons that also lose TMEM16F, have reduction of lipid scrambling, which may reduce their targeting by microglia. This reduction of targeting may thus result in an overall lower inflammatory state that the authors observe [63]. In the study of Batti and colleagues, impaired phagocytosis by conditional KO microglia is observed through an increase of GABAergic neurons and reduction of engulfed material after spinal cord injury [62]. Our results showing an increase of acidification and by extension, phagocytosis, are at odds with the observation from Batti and colleagues. As explained, we use non-physiologic *E. coli*, which further suggests the need to test neuronal material or apoptotic cells in our microglia study. Understanding differences in phagocytic ability and more importantly, lysosomal function will be important to examining the basis for the TMEM16F KO mediated increase of exosome secretion.

Finally, it is also possible that increased MVB fusion events at the plasma membrane are leading to more exosomes. Researchers have shown that various proteins require specific lipid domains for endosomal targeting [150-152]. If TMEM16F plays a role in regulating these domains on the plasma membrane for docking and fusion of MVBs, then knockout of TMEM16F may result in increased exosome release. Better understanding of the mechanism of how TMEM16F mediates or regulates MV or exosome secretion will allow for modulation of EVs through inhibitors or agonists that may help to slow progression of disease and can have huge implications in biomedical research.

## 2.4 FIGURES

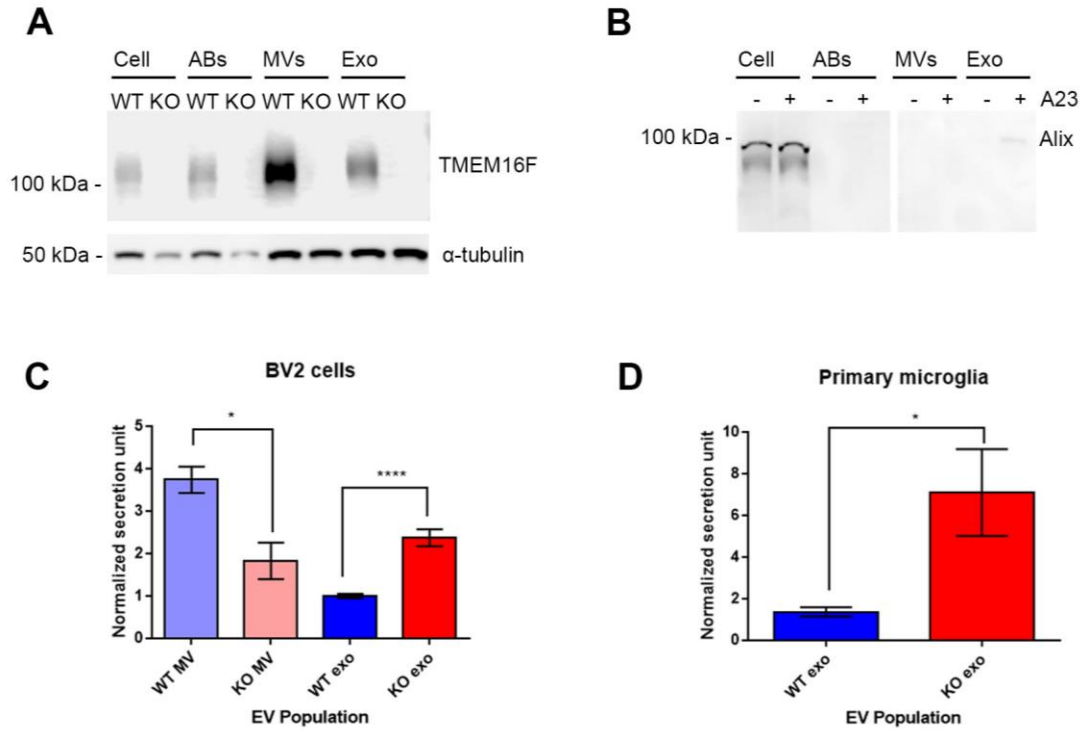


**Figure 2.1. Knockout of TMEM16F from microglia alters extracellular vesiculation.** A) Western blot of extracellular vesicle populations after  $\text{Ca}^{2+}$  stimulation against TMEM16F shows an enrichment in both microvesicles and exosomes. B) Western blot of Alix in  $\text{Ca}^{2+}$ -stimulated EVs. C) Knockout of TMEM16F from BV2 cells produce fewer MVs ( $p = 0.111$ ) and more exosomes ( $p = <0.0001$ ) when counted using ImageStream<sup>x</sup> and Nanosight NTA,  $n = 4$ , x 5 replicates per genotype. MV data is combination of ImageStream<sup>x</sup> and NTA counts. D) TMEM16F KO primary microglia also produce more exosomes upon  $\text{Ca}^{2+}$  stimulation and counting with Nanosight NTA ( $p = 0.0154$ ),  $n = 3$ , x 5 replicates per genotype. Normalized secretion unit for C,D were particle counts/ viable cells/ lowest count. Statistical significance was determined using Mann-Whitney test between BV2 MVs, between BV2 exosomes, and primary exosomes. Error bars in SEM.

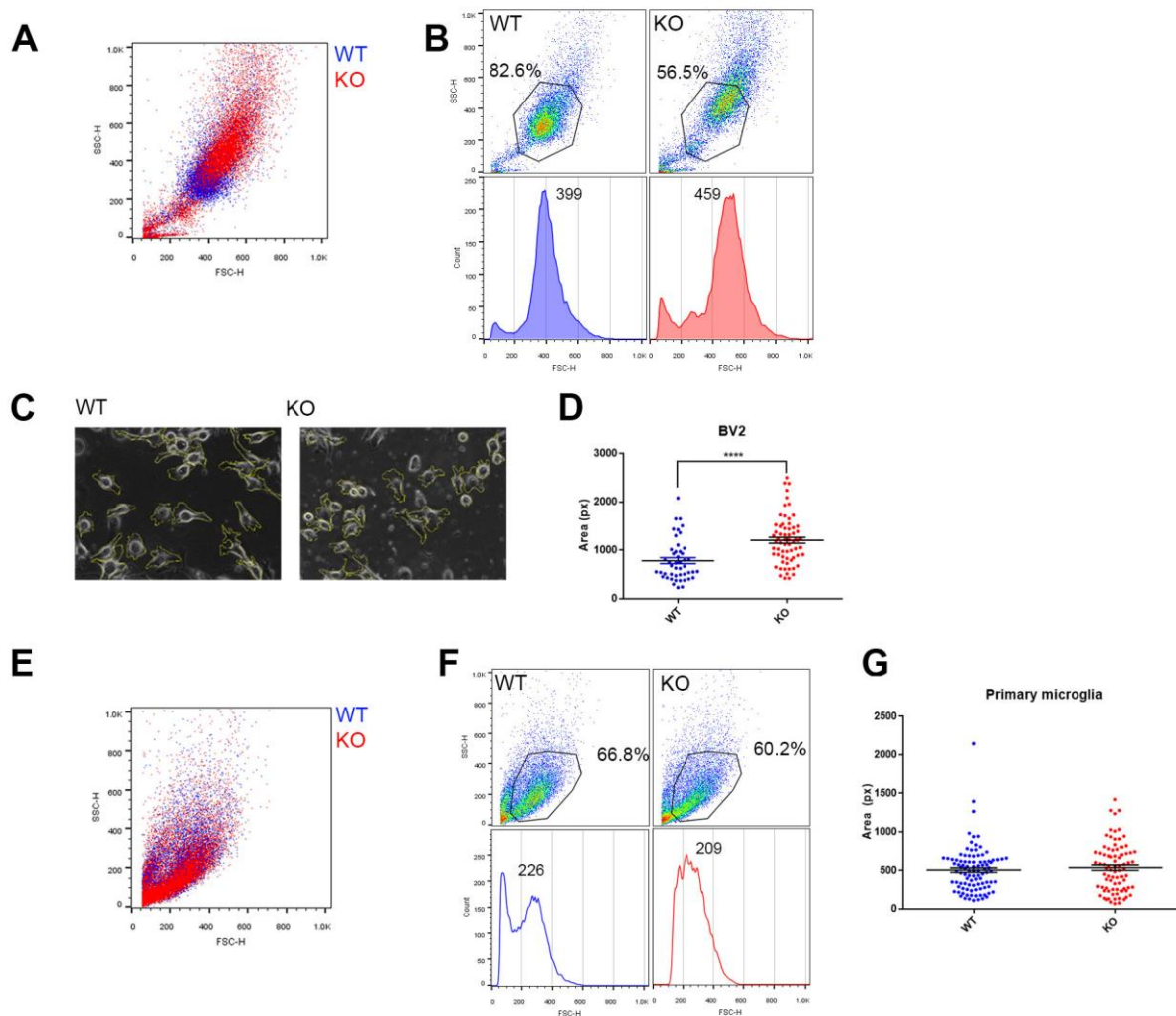


**Figure 2.2 BV2 TMEM16F KO cells are larger than WT, while primary cells exhibit no differences in size.** A) FACS plot depicting WT and TMEM16F KO BV2 cells. B) Gating of WT cells shows KO cells are shifted upwards. C) Representative BV2 cells and trace and D) Quantification of size between TMEM16F KO and WT BV2 cells ( $p < 0.0001$ , Mann-Whitney test,  $n = 50 - 60$  cells. E) FACS plot depicting WT and TMEM16F KO primary microglia. F) Gating of WT cells show no difference between TMEM16F KO microglia. G) Quantification of size based on pixels between primary WT and TMEM16F KO cells ( $n = 80 - 100$  cells). Error bars in SEM.

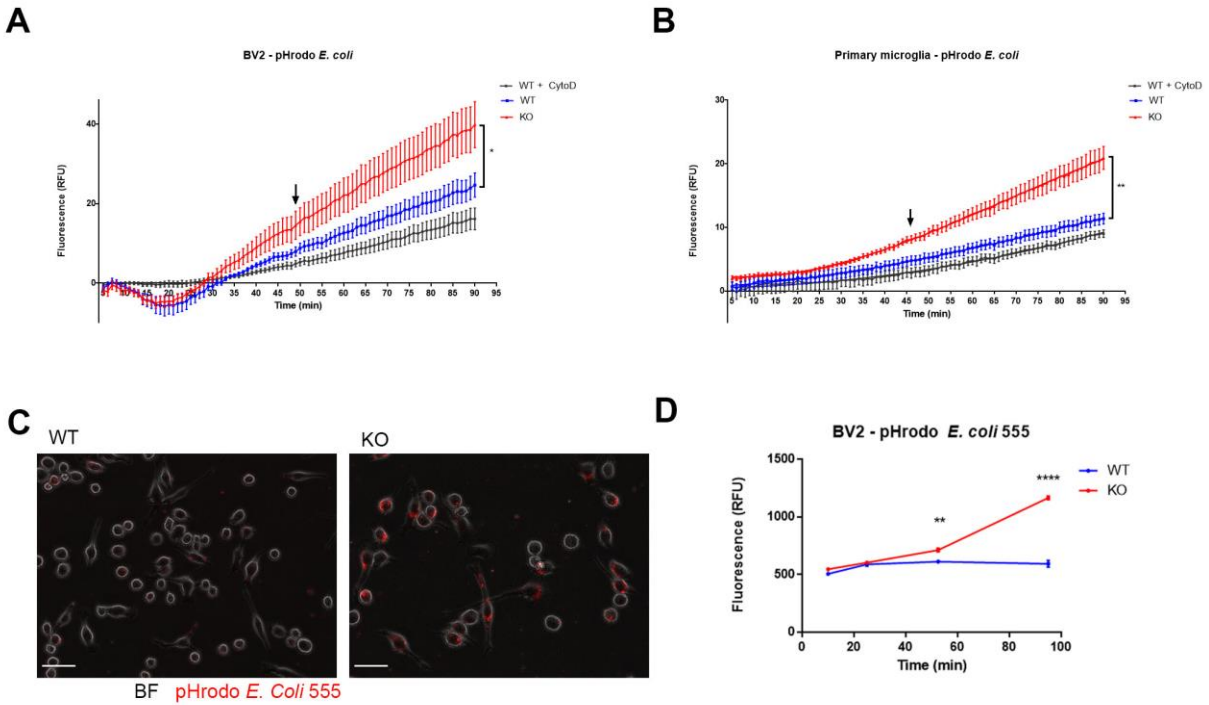


**Figure 2.3 TMEM16F KO cells have enhanced phagocytosis and acidification.** A) Plate reader phagocytosis assay of pHrodo *E. coli* and TMEM16F WT and TMEM16F KO BV2 cells. Cytochalasin D (CytoD) inhibits actin polymerization and suppresses phagocytosis. (n = 4, significance begins at arrow, \* = p < 0.05, two-way ANOVA, Tukey's multiple comparisons test). B) Fluorescence of pHrodo *E. coli* phagocytosis assay with TMEM16F WT and TMEM16F KO primary microglia, n = 3. (Significance begins at arrow, \*\* = p < 0.01, two-way ANOVA, Tukey's multiple comparisons test). C) Representative image of TMEM16F WT and TMEM16F KO BV2 cells with pHrodo Red *E. coli* particles from the end of the experiment. D) Quantification of fluorescence within TMEM16F WT and KO BV2 cells from live microscopy (\*\* p < 0.01, \*\*\*\* p < 0.0001, two-way ANOVA, Sidak's multiple comparisons test). Scale bar, 50  $\mu$ m. Error bars in SEM.

**CHAPTER 3: TMEM16F mediates aberrant neuronal lipid scrambling in the P301S model of tauopathy**



### 3.1 INTRODUCTION

Progressive cognitive dysfunction and neuronal loss are correlated with neurofibrillary tangles (NFTs), which are composed of hyperphosphorylated tau filaments and tau aggregates [113, 120]. In Alzheimer's disease, spreading of tau begins in the entorhinal cortex (Braak stage I/II) and then spreads to the limbic areas including hippocampus (Braak stage III/IV) and finally to the neocortex (Braak stage V/VI) [160]. While AD is a secondary tauopathy, due to A $\beta$  also affecting its pathology, this progression of spread is found in many models of tauopathy [161].

One of which is the P301S (PS19) mouse model that is widely utilized to study tauopathies and their progression of disease [161, 162]. These mice contain a human 1N4R *MAPT* transgene harboring the familial P301S mutation associated with several types of tauopathy [116, 162]. Mice begin to exhibit phenotypic disease pathology as early as 3 months in the form of microgliosis in some brain regions, including white matter and spinal cord [162]. By 6 months, microgliosis is spread to grey matter of the entorhinal cortex, amygdala, and hippocampus [162]. Additionally, neurofibrillary tangles can be found in these brain regions and mice begin to exhibit behavioral memory and learning deficits (Morris water maze and contextual fear conditioning) [162-164]. By 9 months, neuronal loss and ventricle abnormality is significant [165]. The founding line and many studies utilize a C57BL/6 x C3H mixed background. Interestingly, a delay in onset has been reported both in mixed background and in congenic crosses [166, 167].

There are several mechanisms which are known or thought to mediate pathological tau spread. Directly from neurons, naked tau seeds can be directly translocated through the plasma membrane into the extracellular space [168], or enclosed tau can be secreted through exosomes [169] or microvesicles [120, 170, 171]. New studies have also begun to implicate microglia in spreading of soluble tau oligomers, which it can obtain through phagocytosis or endocytosis of neuronal EVs [120]. To first assess the role microglia play in tauopathy, Asai et al. pharmacologically depleted microglia in PS19 mice by using PLX3397, an antagonist against

CSF1R that is crucial receptor required for microglial maturation, replication, and function [107]. They found that removal of microglia resulted in a reduction of the spread of hyperphosphorylated tau [107]. Microglia were able to phagocytose tau and secrete it within exosomes. Furthermore, when exosome machinery in microglia or in the brain was inhibited, tau secretion was equally inhibited [107]. This demonstrated that microglia could worsen tauopathy disease progression and spread of pathological tau through exosomes [107].

## 3.2 RESULTS

### *3.2.i Conditional microglial knockout of TMEM16F in PS19 mice worsens disease progression*

While testing functional roles of TMEM16F in microglia, we discovered that cells lacking TMEM16F release more exosomes, as discussed in **Chapter 2.2.ii**. To assess whether this increased exosome release from microglia has pathological relevance in the context of tauopathy, we crossed TMEM16F flox/flox Cx3cr1-Cre<sup>+</sup> (also referred to as Cre<sup>+</sup> henceforth) mice to PS19<sup>+</sup> mice. Among brain cells, Cx3cr1, the fractalkine receptor, is highly and selectively expressed on microglia and thus its Cre line is often used to study microglia specific knockouts [172]. At 6 months, we observed no differences between PS19<sup>+</sup> Cre<sup>+</sup> and PS19<sup>+</sup> Cre<sup>-</sup> mice in both levels of microgliosis (microglial density within the hippocampus) and that of hyperphosphorylated tau (AT8<sup>+</sup> neurons within the pyramidal layer of CA1) using immunohistochemistry against Iba1 and AT8, respectively (**Figure 3.1A-B**). Additionally, there was no significant difference between PS19<sup>-</sup> and PS19<sup>+</sup> mice in terms of microgliosis, suggesting a delay in onset of disease (**Figure 3.1C**). This falls in accordance with Iba et al. and Zhang et al., as our Cx3cr1-Cre line is on a C57BL/6 background and establishing our PS19 Cx3cr1-Cre line required backcrossing of the PS19 mixed background onto this C57BL/6 one [166, 167].

To allow progression of pathology, we continued to age mice to 7 months and assessed a small n to determine if pathology was present. While not significant due to the small n, there

was a trending difference in both gliosis and hyperphosphorylated tau between PS19- and PS19+ mice (**Figure 3.1 D-E**). Among PS19+ mice, however, the trend seemed less obvious between Cre- and Cre+ (**Figure 3.1D-E**). Despite this, we decided to move forward with behavioral tests to assess memory and learning. Testing for memory and learning would occur after a few weeks which would allow pathology to advance.

### *3.2.ii PS19+ conditional TME1M16F KO mice have partially perturbed behavior*

Mice were first probed for baseline exploratory and anxiety behaviors using the open field test and elevated plus maze, respectively. In open field, total movement was similar among all genotypes, although PS19+ mice spent a larger proportion of time in the center of the field, suggesting less anxious behavior (**Figure 3.2A-B**). This dampening of anxiety was also seen in the elevated plus maze, where PS19+ trended towards spending more time in the open arm, both as more time elapsed towards the end of the trial and when compared to their total distance (**Figure 3.2 C-D**). Elevated plus maze data was slightly confounded by PS19-TMEM16F WT mice exhibiting higher baseline than expected. Additionally, mice exhibited no significant differences in nociception when tested on a hot plate (**Figure 3.2E**). We proceeded to assess various types visual-spatial learning and memory using active place avoidance (APA).

In the APA test, mice are placed onto a rotating wheel with one quadrant providing a foot shock upon entry. Various trials and probes are used to test visual-spatial learning and reference memory [173]. During the training trials, where a shock is active, we found that PS19+ Cre+ mice made more entrances and had shorter latency to enter the shock zone compared to other genotypes (**Figure 3.3**). When the shock was removed and then replaced (probe and reinstatement), PS19+ Cre+ also had a high number of entrances (**Figure 3.3A,C**). This suggested that compared to PS19+ Cre- and PS19- Cre+ mice, microglial knockout in tauopathy worsens learning. Unfortunately, these results are confounded by the poor performance of PS19- Cre- nontransgenic mice which exhibited poor learning in probe and

reinstatement. They had no differences in total movement in open field or hindpaw withdrawal in hot plate, however, suggesting this was not caused by differences in pain perception or impairments in movement (**Figure 3.2A, E**). The large variability across all genotypes, additionally made statistical significance difficult to assess.

### *3.2.iii Tau pathology is exacerbated in PS19 conditional TMEM16F KO mice*

To examine pathology of this cohort at the conclusion of testing (9-10 mo), immunohistochemistry was performed to assess microgliosis and tau hyperphosphorylation. Among PS19+ mice, those deficient in TMEM16F had elevated numbers of AT8+ neurons within CA1 (**Figure 3.4A-B**). PS19+ mice with TMEM16F removed also had increased density of microglia within the hippocampus (**Figure 3.4C-D**). These data showing an exacerbation of disease pathology when TMEM16F is knocked out of microglia suggest intact microglial TMEM16F is important for deceleration of disease progression.

### *3.2.iv Global knockout of TMEM16F reduces disease progression in PS19 mice*

To assess knockout of TMEM16F from all cells, we crossed PS19+ mice with a global TMEM16F KO mouse. As with the conditional knockout, we first assessed pathology at 6 months. Unlike the conditional knockout, however, no further aging was required, as differences were detected at this timepoint. Surprisingly, PS19+ TMEM16F KO mice had no AT8+ neurons within CA1 compared to PS19+ TMEM16F WT mice, which had several (**Figure 3.5A-B**). Additionally, levels of microglia were reduced within the hippocampus of PS19+ TMEM16F KO mice compared to PS19+ mice with TMEM16F (**Figure 3.5 C-D**). As an assessment to determine if these differences also occur earlier, we looked at 3-month-old mice, but observed no significant differences (data not shown). This reduction in pathology observed at 6 months was in stark contrast to the opposite phenotype observed in the conditional knockout mice, where removing TMEM16F from microglia worsens disease progression. This suggested that TMEM16F within other cells may also be affecting disease progression in P301S mice.

Disease progression in tauopathy involves the degeneration of neurons, so it is conceivable that knockout of TMEM16F from neurons is overcoming the effect seen from microglia. Recently, it was found that neurons bearing tau filaments aberrantly expose phosphatidylserine, which targets them for premature efferocytosis by microglia [174]. Efferocytosis is the phagocytosis of dying cells and cellular debris, which often carry the molecular signature of exposed phosphatidylserine [35, 175]. Premature efferocytosis, also known as primary phagocytosis or phagoptosis, is the phagocytosis of living cells [175]. In the brain it is regulated in development with neuronal death in the hippocampus [176] and cerebellum [177], but often becomes misregulated in neurodegeneration [175, 178-180]. Brelstaff et. al demonstrate P301S neurons have an increase in reactive oxygen species, which leads to exposure of phosphatidylserine (PS) [174]. It is possible that this PS exposure is mediated by lipid scramblase TMEM16F and that in the global knockout, neurons with mutant tau are not exposing PS and thus are not being targeted for premature death by microglia.

### *3.2.v TMEM16F KO reduces PS exposure from tau burdened neurons*

To test the role of TMEM16F on lipid scrambling from neurons with or without tau burden, we cultured primary neurons from PS19 TMEM16F mice to obtain TMEM16F WT and KO neurons with or without mutant tau (and thus propensity for tau hyperphosphorylation or aggregation). To assess basal PS exposure in these neurons, cells were labeled with a live neuronal marker (NeuroFluor NeuO) and probed with Annexin V, which binds PS, and a Caspase 3 reporter (NucView 405) to exclude apoptotic cells from analysis. PS19+ TMEM16F WT neurons had significantly higher PS signal per neuron, compared to both PS19- genotypes as well as PS19+ TMEM16F KO neurons (**Figure 3.6A-B**). It is possible that TMEM16F is affecting cell death and that some neurons that have PS exposure may be excluded from analysis. However, we saw that all genotypes had similar high percentages of living cells (98-

99%), suggesting this was not the case (**Figure 3.6C**). Together, these data demonstrate TMEM16F is mediating PS exposure in tau burdened neurons.

PS exposure is linked to total hyperphosphorylated tau burden [174]. It is possible that TMEM16F affects this tau burden within neurons and that its knockout reduces it, which may result in the lower PS exposure observed. To see if neurons with or without TMEM16F differed in the amount of resulting tau burden, we stained neurons for hyperphosphorylated tau and looked for differences between genotypes. Preliminary assessment of the proportion of AT8+ neurons to total neurons indicate similar results for both TMEM16F WT and KO neurons, which suggests the reduction in PS exposure from TMEM16F knockout is not due to an altered expression of the P301S transgene (data not shown).

### *3.2 vi Microglia have fewer interactions with tau burdened TMEM16F KO neurons*

To begin to assess how tau burden and thus PS exposure of neurons correlates to phagocytosis by microglia, we added WT microglia into primary neuronal cultures. Preliminary assessment shows a trend that after three days, microglial interaction with AT8+ neurons is reduced by TMEM16F removal from neurons (**Figure 3.7**). This is in accordance with research showing that PS exposure allows for targeting by microglia [181]. Subsequent analysis is needed to assess efferocytosis.

## **3.4 DISCUSSION**

Despite expression in almost all cells of the body, the role of TMEM16F in the brain and central nervous system (CNS) is largely unknown. Thus far, only three studies have explored TMEM16F in the CNS. Two have demonstrated the role of TMEM16F in regulating spinal cord microglia in neuropathic pain states [62] and spinal cord injury [63] and one has examined neurons after cerebral ischemia in relation to scrambling ability [64]. Because of TMEM16F implication in both lipid scrambling and extracellular vesiculation, there exist many more aspects to explore.

Our data adds, in part, to a growing body of research showing extracellular vesicles play an important role in the spreading of pathological proteins. While proteins secreted directly from dying or overwhelmed cells are able to be taken up by neighboring ones, those encased in extracellular vesicles are afforded additional protection from degradation, which can allow for more time in the extracellular space and longer range of spread [148]. In tauopathies, where hyperphosphorylated tau oligomers elicit prion-like behavior, microglial exosomes are one such mechanism of their spread [107, 116]. Our discovery that knockout of TMEM16F in microglia increased release of exosomes prompted us to examine a possible functional consequence in P301S mice. We found that conditional knockout of TMEM16F from microglia exacerbates pathology and slightly impairs memory and learning behavior in these mice. Surprisingly, complete knockout of TMEM16F resulted in a reduction of pathology, which suggested the detrimental effects of microglial knockout of TMEM16F were overcome by beneficial effects of another cell type. Aberrant lipid scrambling from neurons and thus exposure of PS has been implicated in neuronal loss during neuroinflammation [174, 179, 180, 182]. To see if TMEM16F was mediating this exposure, we examined P301S neurons with or without TMEM16F and found that knockout reduces PS exposure that becomes elevated with tau burden. Preliminary assessment of neuronal/ microglial cocultures suggests this reduction in PS exposure of TMEM16F KO neurons also reduces interactions with WT microglia, supporting the assertion that aberrant PS exposure from neurons may lead to their early death by microglia. Collectively, these findings demonstrate multifaceted roles of TMEM16F in extracellular vesiculation and in lipid scrambling in brain cells in tauopathy.

Our PS exposure data is confirmed by a recent study examining neuronal TMEM16F after cerebral ischemia. They found that knockdown of TMEM16F in neurons reduces PS exposure after ischemia and this reduction helps to prevent neuronal loss by preventing microglial targeting [64]. Previously, Brelstaff and colleagues demonstrated that reactive oxygen species (ROS) are increased in P301S+ neurons and that this increase corresponds to PS

exposure [174]. It is known that ROS and  $\text{Ca}^{2+}$  as second messengers to one another and have significant cross talk [183]. ROS is known to activate both ryanodine receptors (RyRs) and  $\text{IP}_3$  receptors ( $\text{IP}_3\text{Rs}$ ) on the endoplasmic reticulum, which allow for  $\text{Ca}^{2+}$  release and subsequent store-operated  $\text{Ca}^{2+}$  entry [183, 184]. Increased intracellular  $\text{Ca}^{2+}$  can then enter mitochondria and increase respiratory chain activity which in turn, leads to elevated ROS [183]. Both RyR and  $\text{IP}_3\text{R}$  function at internal  $\text{Ca}^{2+}$  stores within hippocampal neurons and other central neurons [185]. Additionally, both  $\text{Ca}^{2+}$  and ROS can act as inhibitors of flippases such as the P4-ATPase ATP11C, which with otherwise move phosphatidylserine from the outer to inner leaflet [35, 175].

It has been reported separately that in both human Alzheimer's patients and mouse models of tauopathy, there is  $\text{Ca}^{2+}$  dyshomeostasis [186-188]. In models where human Tau (hTau), V337M 2N4R hTau, or P301L 0N4R hTau have been overexpressed in neuronal cells *in vitro* [188] or in mice,  $\text{Ca}^{2+}$  is elevated [186, 189]. The latter two mutations of human tau affect microtubule binding and, specifically, the P301L 0N4R mutation utilized in the JNPL3 mouse model of tauopathy heavily phenocopies the P301S (1N4R) model used in our current study [161, 162, 186, 187, 189]. Finally, ROS stimulation with tert-butyl hydroperoxide (tBHP) in HEK cells overexpressing TMEM16F has been shown to increase PS exposure [190]. Taken together, it is certainly conceivable that tau burden within neurodegenerative neurons lead to ROS, which increases cytoplasmic  $\text{Ca}^{2+}$ , activates TMEM16F, and results in lipid scrambling and exposure of phosphatidylserine which can then target the cell for premature efferocytosis. The prospect of TMEM16F inhibition to reduce pathology in neurodegeneration presents an exciting future therapeutic strategy. However, our data also shed light on an opposing mechanism from microglia that requires attention.

While future studies need to assess the bioactive content of exosomes from TMEM16F knockout microglia, it is conceivable they play a role in tau pathology, given microglial exosomes are known carriers of tau oligomers in tauopathy [107]. Our data in microglial conditional knockout mice support this hypothesis, in that mice which have microglia that



secrete more exosomes have a worsening of tauopathy. It was thus surprising to see a reduction in pathology when TMEM16F was removed from all cells. One potential mechanism of tau secretion from neurons is through microvesicle release, as it has also been found in cerebral spinal fluid of Alzheimer's patients [171, 191]. As neurons become overburdened with tau oligomers and filaments, they begin to secrete these species into the extracellular space, where they can be taken up by microglia [120]. Aggregation of tau forms higher order oligomers and this type of oligomerization has been shown to be targeted towards the plasma membrane [147, 192]. Because microvesicles (MVs) are released from the plasma membrane and tau has been discovered within neuronal MVs in disease patients, it is likely neurons may partially spread tau with microvesicles. As Brelstaff et al. and our data have also demonstrated, tau burden also leads to PS exposure [174], which additionally can result in neuronal loss in pathology [165].

One possible explanation for our finding of global TMEM16F knockout mice, is that in addition to PS exposure being prevented from tau burdened neurons, tau secretion may vary depending on cell type. In neurons where tau forms higher order oligomers and fibrillary tangles, these species may be released through MVs [147, 192] and in microglia, where tau is presumably broken up into smaller oligomers, it may be spread through exosomes [107, 120]. If TMEM16F affects vesiculation from neurons as it does in all other cell types that have been studied, knockout would presumably reduce MV release. In the conditional microglial knockout, neurons with TMEM16F intact could still secrete tau fibrils through MVs and also expose PS owing to increased ROS. The increase in exosomes from TMEM16F KO microglia, which may contain lower order tau oligomers would exacerbate pathology. In the global knockout, however, where both neurons and microglia are lacking TMEM16F, neurons would be deficient in MV release and also PS exposure. This would not only reduce possible release, but also subsequent uptake, of tau containing MVs by other neurons and also microglia. Preventing the opportunity of microglial uptake would in turn dampen the release of tau-containing exosomes, despite these microglia being capable of increased exosome release. In addition, because tau

burdened neurons do not aberrantly expose PS, they are not targeted for efferocytosis by microglia, further preventing exacerbation of pathology.

While complex, this proposed mechanism may correspond to the timeline of pathology we see in our mouse study. We were able to see reduction in pathology from our global knockout mice by 6 months, but we were unable to see differences between microglial TMEM16F cKO mice at 6 and 7 months. It may take longer to separate out differences from increased microglial tau spreading as compared to presumed deficient neuronal tau release in microvesicles. Neuronal loss in P301S mice is usually not seen until late stage in disease progression around 9 months [162, 165]. Thus, protective effects of TMEM16F knockout in neurons may first involve a reduction of MV release and later the prevention of lipid scrambling and thus reduction of premature efferocytosis and neuronal loss.

Our findings, in conjunction with other studies, establish an exciting framework to study manipulation of pathological tau release, which may aid in development of future therapeutics not only in tauopathy but also other neurodegenerative disease.

### 3.5 FIGURES

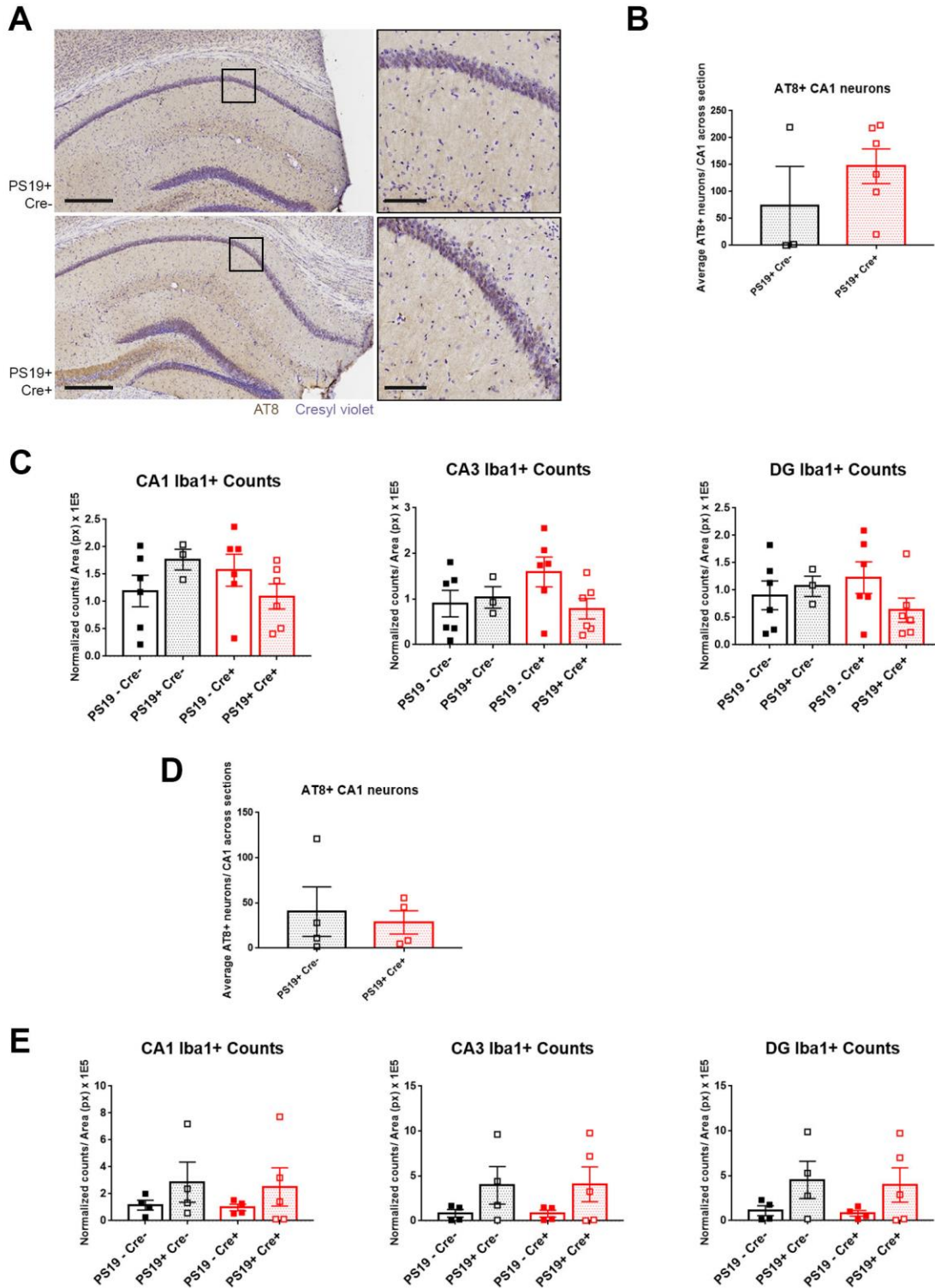


**Figure 3.1 7-month-old, but not 6-month-old PS19 Cx3cr1-Cre mice display differences in disease pathology.** A) Representative images of AT8 immunostaining of hyperphosphorylated tau in the hippocampus and CA1 (inset) in 6-month-old PS19+ Cre- and Cre+ mice. Scale bar,

300  $\mu\text{m}$  for hippocampus and 80  $\mu\text{m}$  for inset. B) Quantification of AT8+ neurons within CA1 pyramidal layer in PS19+ Cre-, n = 3 and PS19+ Cre+ 6 mice, n = 6; 3-4 hippocampal sections/ mouse. C) Quantification of number of microglia per area (count / area(px) x 1E5) in the hippocampal regions CA1, CA3, and dentate gyrus (DG) of 6-month-old PS19- Cre-, n = 6 mice; PS19- Cre+, n = 5; PS19+ Cre-, n = 3; PS19+ Cre+, n = 6. D) Quantification of average # of AT8+ neurons in CA1 of 7-month-old PS19+ Cre- and PS19+ Cre+ mice, n = 3 each. E) Quantification of microglia per area (count/ area (px) x 1E5) in the hippocampus in PS19- Cre-, PS19- Cre+, PS19+ Cre-, and PS19+ Cre+, n = 3 mice each. No statistical significance, but trending difference between PS19- and PS19+ mice. Error bars in SEM.

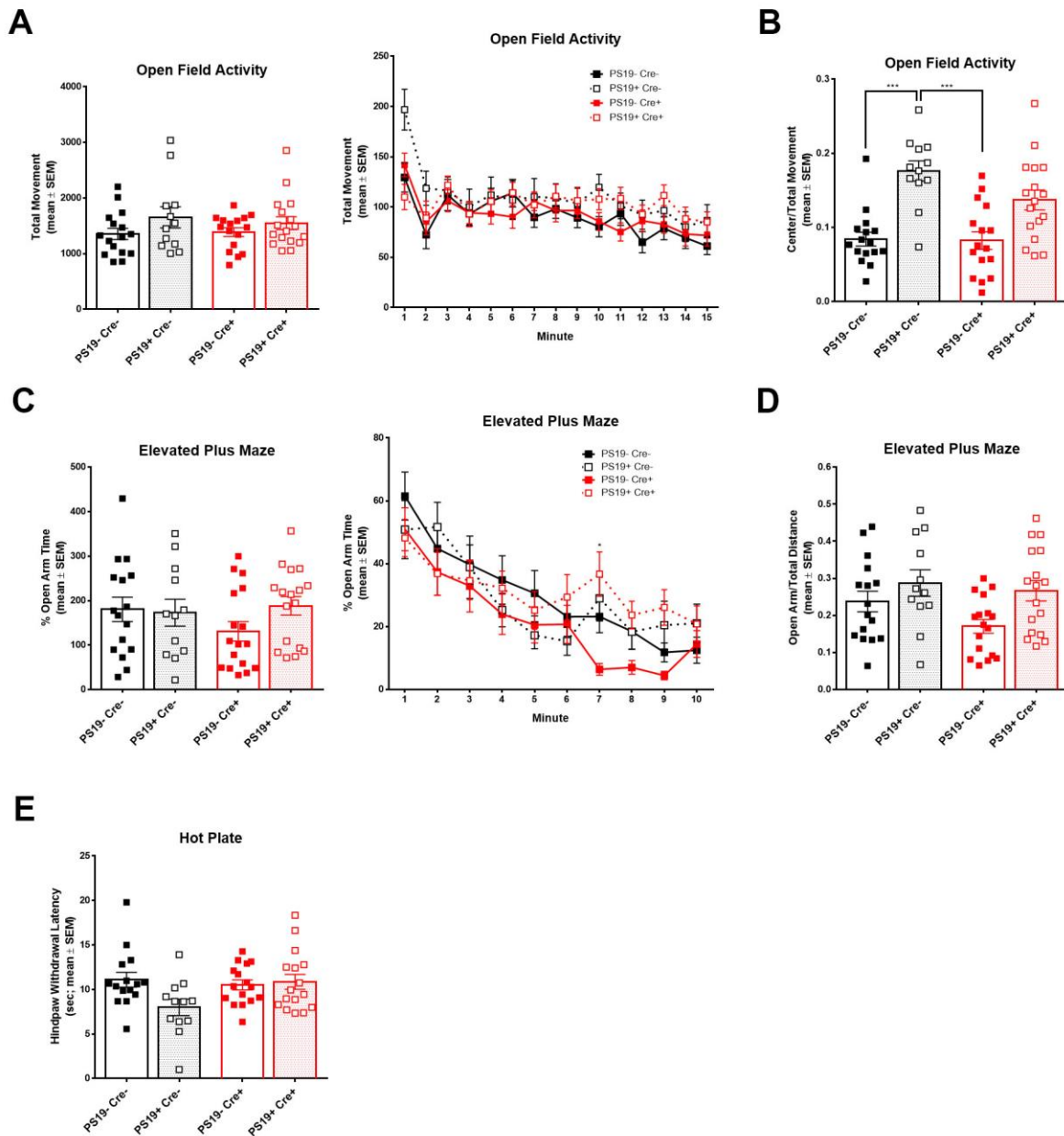


**Figure 3.2 Baseline activity and anxiety slightly perturbed.** A) Open field total movement and total movement by time in 7- to 8-mo in PS19- Cre-, n = 16 mice; PS19+ Cre-, n = 16; PS19- Cre+, n = 13; PS19+ Cre+, n = 17. B) Proportion of movement within center of field/ total movement between mice in (A). (\*\*\*\* =  $p < 0.001$ , Kruskal-Wallis test, Dunn's multiple comparisons test). C) Percent within open arm of EPM over total time and per minute during trial in PS19- Cre-, n = 16 mice; PS19+ Cre-, n = 17; PS19- Cre+, n = 13; PS19+ Cre+, n = 17. D) Proportion of distance within open arm to total distance in mice in (C). E) Latency to hindpaw removal in hotplate test in PS19- Cre-, n = 16 mice; PS19+ Cre-, n = 17; PS19- Cre+, n = 13; PS19+ Cre+, n = 17. Error bars in SEM.

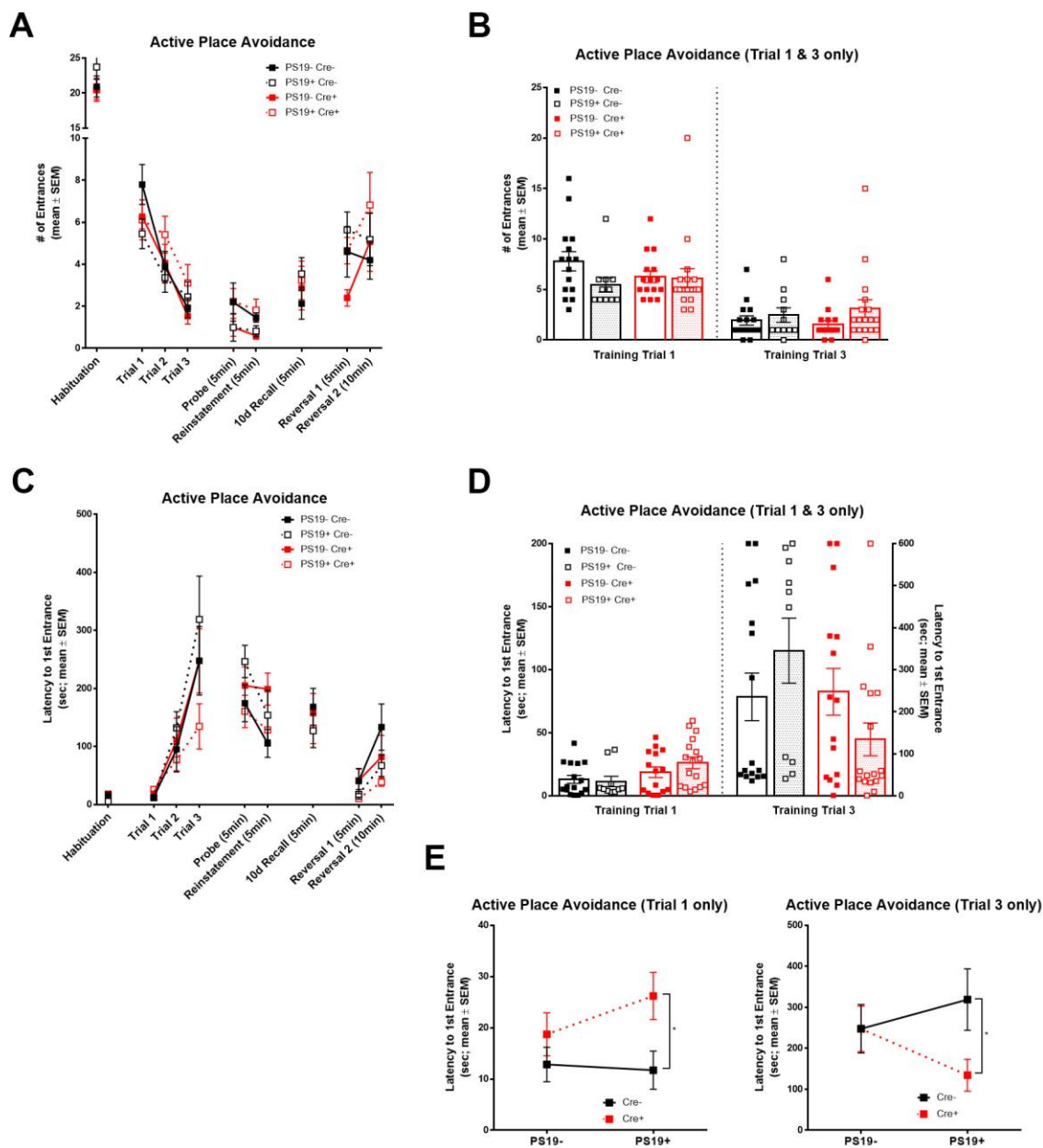


**Figure 3.3 Modest impairment to visual/ spatial learning in PS19+ conditional TMEM16F KO mice.** A) Number of entrances into shock quadrant for all trials (habituation, three trials, probe (shock removed), reinstatement (shock reinstated), 10d recall, reversal (shock moved to opposite quadrant), and trial 2 of new quadrant in PS19- Cre-, n = 16; PS19+ Cre-, n = 11; PS19- Cre+, n = 15; PS19+ Cre+, n = 17. B) Number of entrances into shock quadrant in trials 1 and 2 for mice in (A). C) Latency to first entrance into shock quadrant over trials detailed in (A) for mice in (A). D) Latency to first entrance for trial 1 and trial 3 for mice in (A). E) Two way design latency to first entrance in trial 1 ( $p = 0.183$ , two-way ANOVA) and trial 3 ( $p = 0.0476$ , multiple t tests) for mice in (A). Error bars in SEM.



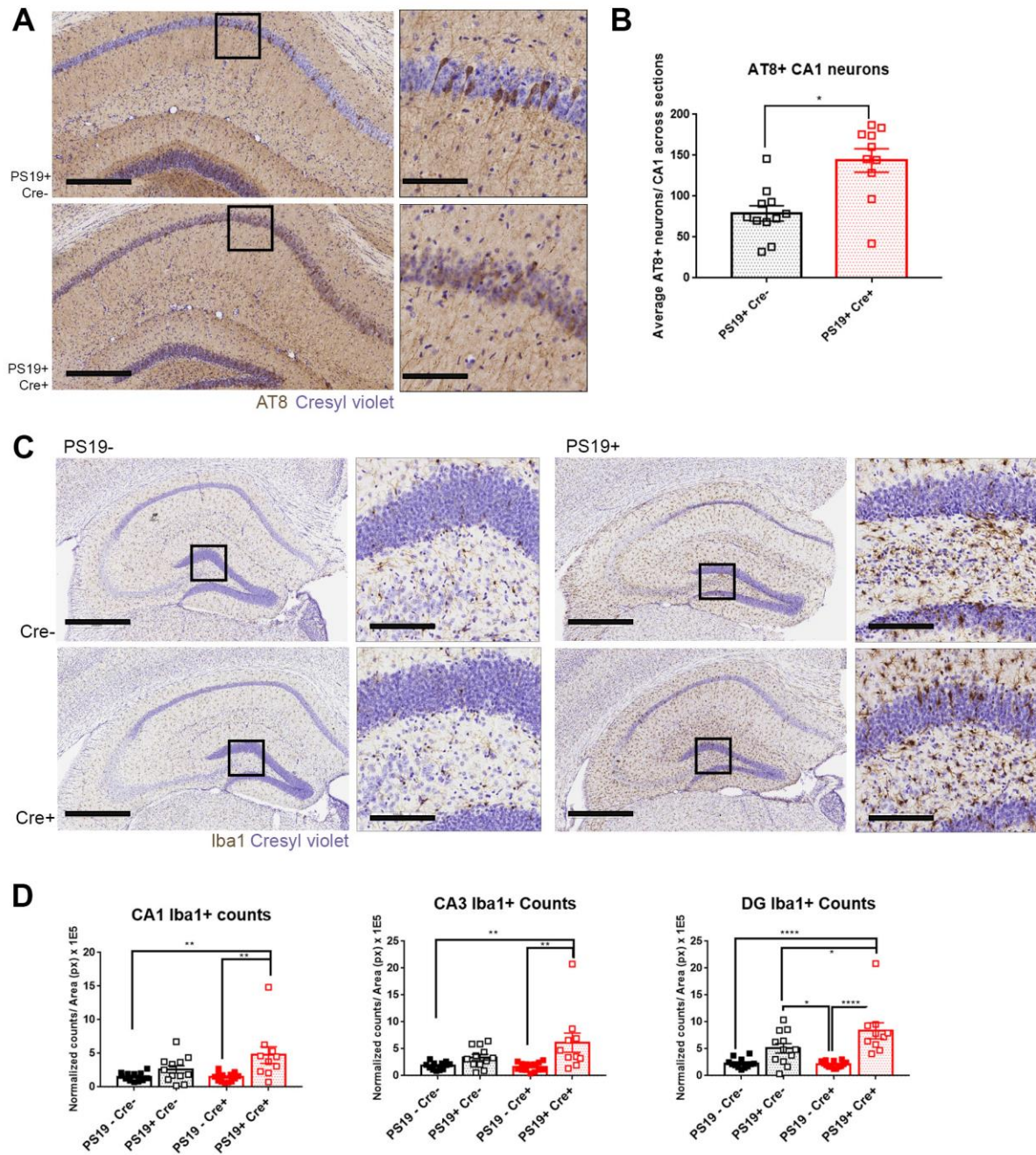


**Figure 3.4 TMEM16F KO in microglia worsens pathology in tauopathy.** A) Representative images of AT8 immunostaining of hyperphosphorylated tau in the hippocampus and CA1 (inset) in 9- to 10-month-old PS19+ Cre- and Cre+ mice. Scale bar, 300  $\mu$ m for hippocampus and 80  $\mu$ m for inset. B) Quantification of AT8+ neurons within CA1 pyramidal layer in PS19+ Cre-, n = 11 and PS19+ Cre+, n = 10 mice; 3-4 hippocampal sections/ mouse. (p = 0.002, Mann-Whitney test) C) Representative images of Iba1 immunostaining of microglia in the hippocampus and DG (inset) of 9- to 10-month-old PS19- Cre-, PS19- Cre+, PS19+ Cre-, and PS19+ Cre+ mice. Scale bar, 300  $\mu$ m for hippocampus and 80  $\mu$ m for inset. D) Quantification of number of microglia per area (count / area(px) x 1E5) in the hippocampus of 9 to 10-month-old PS19- Cre-, n = 12 mice; PS19- Cre+, n = 14; PS19+ Cre-, n = 12; PS19+ Cre+, n = 10. (\*\* = p < 0.01, \*\*\*\* = p < 0.0001, Ordinary one-way ANOVA, Tukey's multiple comparisons test). Error bars in SEM.

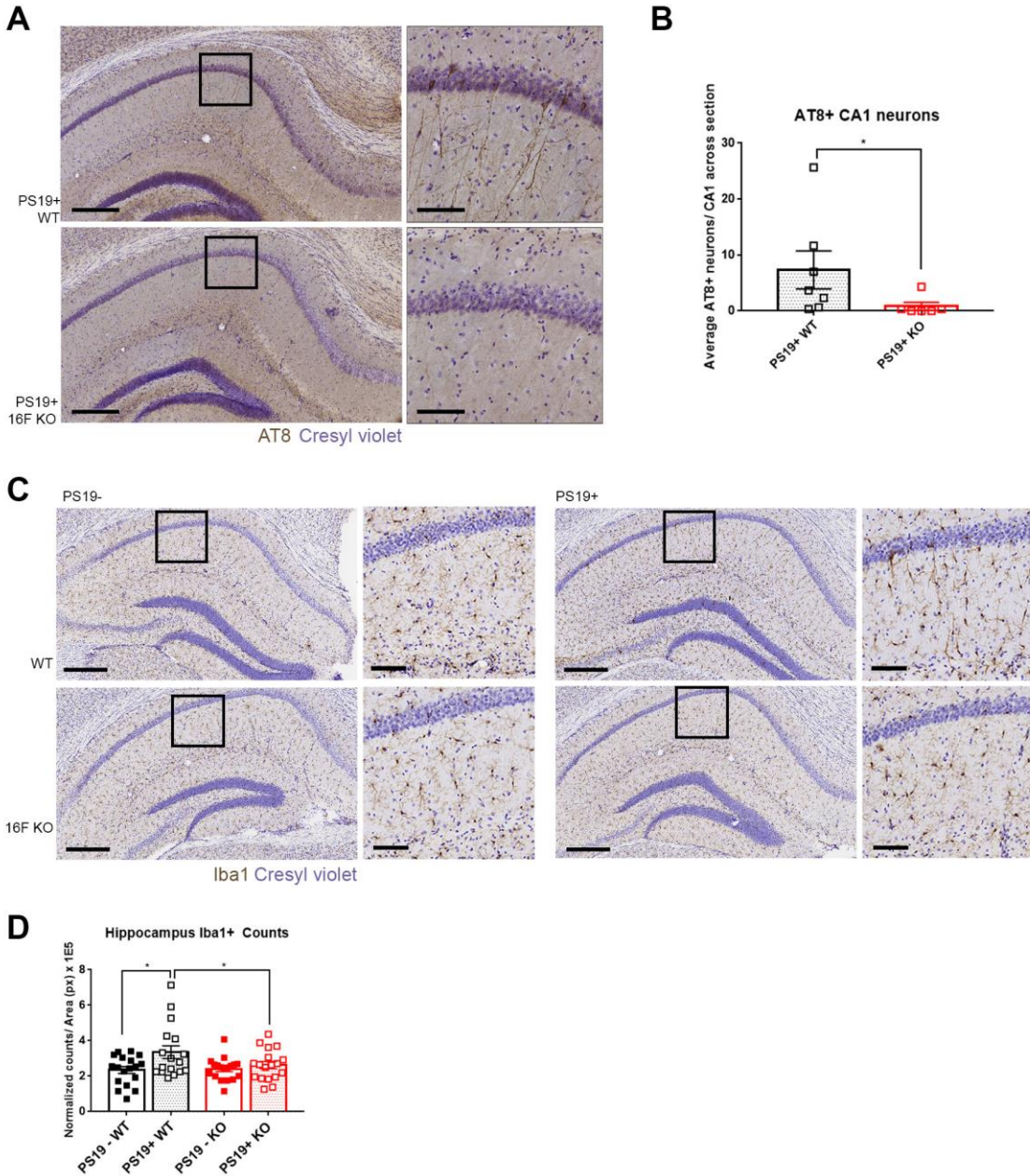


**Figure 3.5 Complete TMEM16F knockout reduces progression of disease. A)**

Representative images of AT8 immunostaining of hyperphosphorylated tau in the hippocampus and CA1 (inset) in 6-month-old PS19+ TMEM16F WT and TMEM16F KO mice. Scale bar, 300  $\mu$ m for hippocampus and 80  $\mu$ m for inset. B) Quantification of AT8+ neurons within CA1 pyramidal layer in PS19+ WT, n = 7 and PS19+ KO mice, n = 6; 3-4 hippocampal sections/mouse. ( $p = 0.03$ , Mann-Whitney test) C) Representative images of Iba1 immunostaining of microglia in the hippocampus and CA1 (inset) of 6-month-old PS19- TMEM16F WT, PS19- TMEM16F KO, PS19+ TMEM16F WT, and PS19+ TMEM16F KO mice. Scale bar, 300  $\mu$ m for hippocampus and 80  $\mu$ m for inset. D) Quantification of number of microglia per area (count / area (px) x 1E5) in the hippocampus of 6-month-old PS19- TMEM16F WT, PS19- TMEM16F KO, PS19+ TMEM16F WT, and PS19+ TMEM16F KO mice, n = 6 per genotype. (\* =  $p < 0.05$ , Ordinary one-way ANOVA, Tukey's multiple comparisons test). Error bars in SEM.



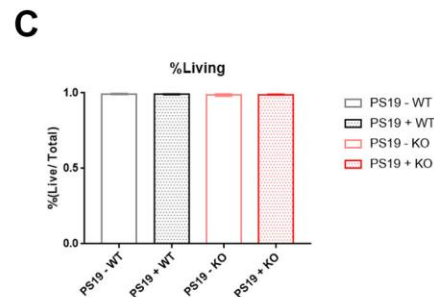
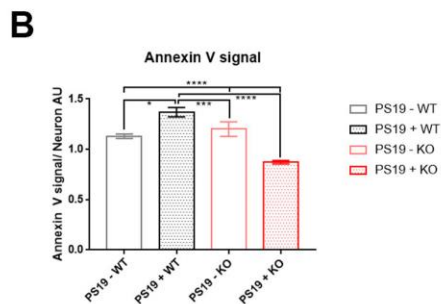
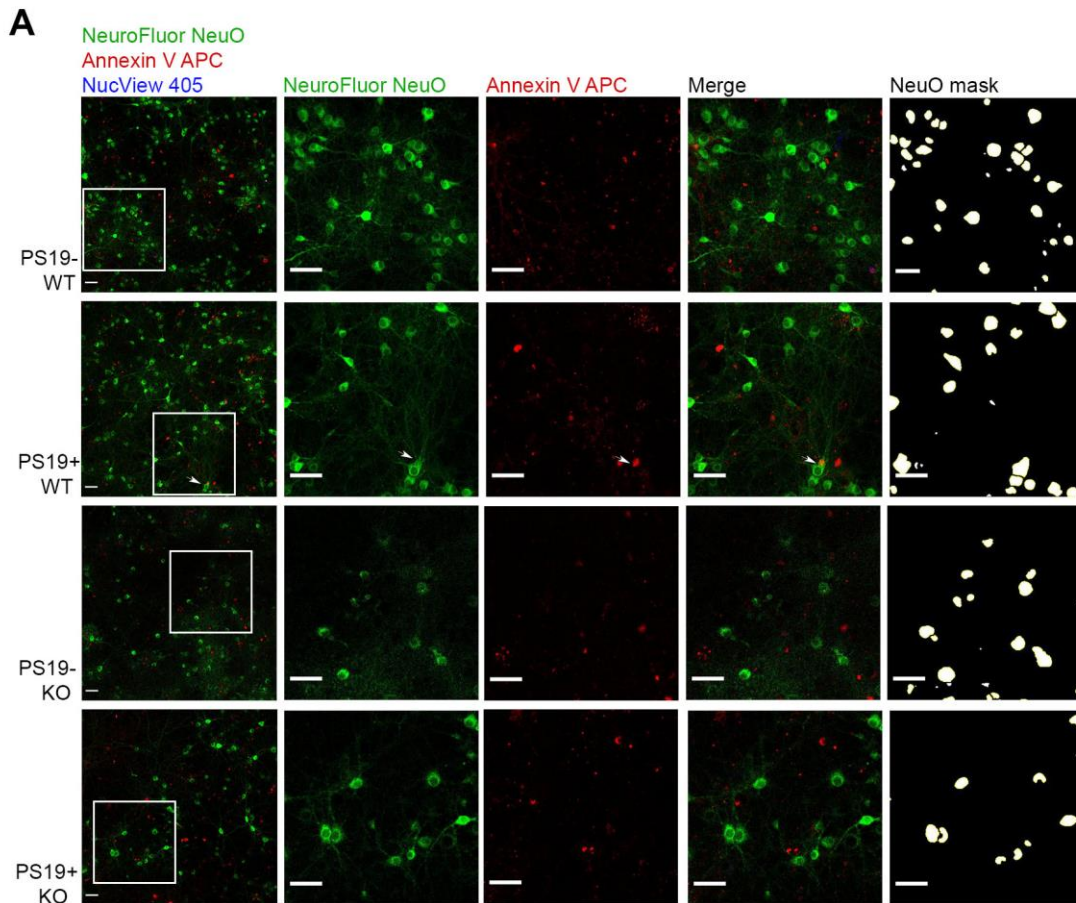


**Figure 3.6 TMEM16F KO reduces PS exposure in P301S neurons.** A) Representative images of NucView 405 (Caspase 3 activity), NeuroFluor NeuO (neurons), and Annexin V (exposed phosphatidylserine) immunostaining in primary PS19- TMEM16F WT, PS19+ TMEM16F WT, PS19- TMEM16F KO, and PS19+ TMEM16F KO neurons. Scale bar, 50  $\mu$ m in all images. B) Quantification of average Annexin V fluorescence per live cell per image of PS19 TMEM16F neurons; 100 – 300 cells per image, 41 - 45 images per genotype. Live cell regions of interest were created by removing NucView 405 masks from those of NeuroFluor NeuO. (\* =  $p < 0.05$ , \*\*\*\* =  $p < 0.0001$ , Kruskal-Wallis test, Dunn's multiple comparisons test). C) Quantification of living cells [live (NeuroFluor NeuO)/ total cells] between PS19- TMEM16F WT, PS19+ TMEM16F WT, PS19- TMEM16F KO, and PS19+ TMEM16F KO neurons. Error bars in SEM.

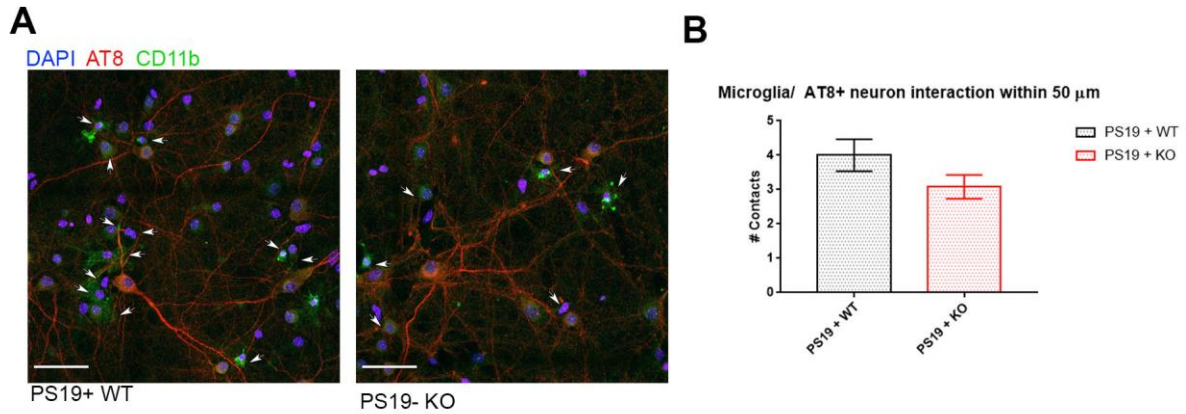


**Figure 3.7 Microglia have fewer interactions with AT8+ TMEM16F KO neurons.** A) Representative images of AT8 and CD11b immunostaining of hyperphosphorylated tau and microglia, respectively, in PS19+ TMEM16F WT and PS19+ TMEM16F KO neurons + WT microglia coculture. B) Quantification of microglia contact within 50  $\mu$ m of AT8+ neuronal cell bodies in PS19+ TMEM16F WT and PS19+ TMEM16F KO neuron-microglia cocultures,  $n = 25$  AT8+ cells per genotype ( $p = 0.17$ , Mann-Whitney test). Error bars in SEM.

## **CHAPTER 4: CONCLUDING REMARKS**

## 4.1 CONTRIBUTIONS TO THE FIELD

The work described in these chapters provides novel insight into the function of TMEM16F in physiology, in relation of extracellular vesiculation and in disease, in the context of tauopathy.

In Chapter 2, we assessed the role that TMEM16F plays in microglia. We found that knockout of TMEM16F results in decreased microvesicle (MV) release, as has been reported for all other cell types studied, as well as increased release of exosomes. We began to probe this mechanism and ruled out acidification impairment or increased volume as causes for this increase exosome formation/ release. This provides insight into the interconnectivity of the endolysosomal pathway, the plasma membrane, and the interplay between different extracellular vesicles, their biogenesis, and their release.

In Chapter 3, we looked at the functional consequence of increased microglial exosome release in the context of tauopathy, where microglial exosomes have been shown to mediate spread of mutant tau oligomers [107]. We found that knockout of TMEM16F in microglia exacerbated disease pathology, consistent with an increase of exosomes which could further spread toxic tau species to neurons. In the complete removal of TMEM16F from all cells, however, we found a reduction in pathology, suggesting other cell types were being differentially affected by TMEM16F removal. Given their prominence in neurodegenerative disease and a recent study examining aberrant phosphatidylserine (PS) exposure [174], we assessed the role of TMEM16F in neurons to expose PS and found that tau burdened neurons with TMEM16F knocked out no longer aberrantly exposed PS. These neurons had fewer interactions with microglia further supporting a body of research showing exposure of PS can lead to targeting and death of living cells. These experiments demonstrate a multifaceted role of TMEM16F depending on cell type in the tauopathy brain. In tauopathy, microglia might utilize TMEM16F's scramblase ability to properly regulate exosome formation/ release, while neuronal TMEM16F may mediate neuronal loss through PS exposure.

## 4.2 FUTURE DIRECTIONS

### *4.2.i Mechanistic insights into TMEM16F and extracellular vesiculation*

Our work reveals exciting new understanding of TMEM16F in regulation of not just MVs, but also exosomes. Extracellular vesicles have physiological functions in almost every cell type across the body. The ability to regulate their secretion can have huge implications in health and disease.

Future directions of exploring the role of TMEM16F in extracellular vesiculation are to examine how it can regulate exosome formation. At the plasma membrane, lipid domain alteration both induces curvature and recruits proteins able to aide in fission [193]. Given the role of TMEM16F to alter lipid composition on a particular leaflet of the bilayer, it seems likely this is a mechanism for TMEM16F-mediated membrane blebbing and release of MVs. Exosome machinery utilizes much of the same processes used in the formation of ILVs and MVBs. Thus, next steps can involve using various forms of microscopy to quantify ILV and MVB formation after  $\text{Ca}^{2+}$  stimulation. Assessing lysosomal function through receptor degradation assays can further pinpoint where TMEM16F may be acting. Furthermore, additional microscopy approaches can be utilized to assess MVB fusion at the plasma membrane.

As with almost every other protein, TMEM16F is not unifunctional, so it will be important to examine what exactly is being acted upon and how knockout will affect that process and downstream processes as well. Additionally, our study focuses on only microglia after  $\text{Ca}^{2+}$  stimulation. It will be important to assess EVs in other cell types with various stimulations to see if the results are consistent and under what conditions they can be replicated. The cargo and formation of EVs varies dramatically depending on cell type and stimulation, so TMEM16F may also exhibit varying regulatory abilities. Studying TMEM16F and its functions will not only prove useful for understanding its ability as a phospholipid scramblase but also shed light on how it may be targeted for future therapeutics.

#### *4.2.ii Targeted TMEM16F manipulation may prove therapeutic in tauopathy*

Tauopathies, both primary and secondary in nature, present a huge societal burden and impending health and economic crisis as the population of the world ages and their lifespan increases [109]. Our research expands upon previous studies showing that tau can be spread by extracellular vesicles. We must, however complete our validation. Immediate future steps are to further show that microglia can contribute to neuronal loss of tau burdened neurons with TMEM16F intact. To solidify that TMEM16F is responsible for PS exposure, we can utilize TMEM16A/ F inhibitors. Furthermore, to better grasp causes leading to activation of TMEM16F to induce this PS exposure, we can test ROS stimulation on TMEM16F KO neurons and also test anti-ROS antioxidants in tau burdened neurons with or without TMEM16F. Understanding how PS exposure is altered and how TMEM16F affects it may help prevent neuronal loss and decelerate neurodegeneration.

When analyzing the timeline of pathology in P301S mice with conditional microglial or global knockout of TMEM16F, we hypothesized that other factors beside neuronal PS exposure may be at play. It is possible that higher order tau oligomers are packaged within neuronal MVs and that secretion of these MVs precedes aberrant PS exposure. If true, then TMEM16F knockout would first influence neurons by reducing their ability to produce MVs and thus decelerate spreading of tau earlier in disease. Knockout microglia lacking TMEM16F would be unable to take up these tau filled MVs (that were never released) and thus could not process them into smaller oligomers to spread with their exosomes. Tackling this hypothesis will require isolation of different populations of vesicles from neurons and microglia but could prove exciting if pathological tau is indeed spread through different vesicle populations depending on cell type.

Our study and future work into EVs in the spreading of tau oligomers helps provide support and lay the groundwork for future studies into assessing how other pathological proteins in neurodegenerative disorders may spread via brain cells throughout the course of disease. Furthermore, apart from spreading of pathological proteins in the brain, cells across the entire

body have been implicated in secretion of toxic proteins. Our studies can be applied to other pathological states and hopefully understanding the role of TMEM16F in extracellular vesicle generation and release can guide future development of therapeutics to slow or halt disease.

## **CHAPTER 5: MATERIALS AND METHODS**



## Animals

TMEM16F complete knockout and TMEM16F flox/flox mice were generated as described previously (Yang et al., 2012) and backcrossed to C57BL/6 background for two to four generations. For TMEM16F complete knockout mice, backcrossing beyond three or four generations resulted in nonviable knockout mice, so these mice were kept on an F1 C57BL/6 / 129S1 background for het x het crossings. TMEM16F flox/flox were bred with Cx3cr1-Cre mice. P301S tau (PS19) breeder males were purchased from Jackson laboratory (B6;C3-Tg(Prnp-MAPT\*P301S)PS19Vle/J) and crossed to TMEM16F flox/flox Cx3cr1-Cre mice or TMEM16F complete KO mice.

All animal procedures were approved by the UCSF Institutional Animal Care and Use Committee and performed according to the guidelines provided.

## CRISPR/ Cas9 Knockout of TMEM16F in BV2 cells

Using CRISPR/ Cas9 technology, TMEM16F was knocked out of the BV2 cell line (gift provided by the Gan lab). sgRNA guides were designed using <https://crispr.mit.edu> and checked for cross reactivity. The human mutation in Scott Syndrome results in a stop codon in exon 2/3, so we sought to induce a mutation either here or in exon 1/2 (numbering varies depending on isoform).

**Table 5.1. CRISPR/ Cas9 sgRNA guides**

Targeted exon and PAM	sgRNA guides
<b>Exon 1:</b> GCTGGAGGAGGACGACGATG <b>AGG</b>	CACCGGAGGAGGACGACGATG
	AAACCATCGTCGTCCTCCTCC
<b>Exon 2, reverse:</b> AGGTGGGGCAGACAATTGTCT <b>TGG</b>	CACCGTGGGGCAGACAATTGTC
	AAACGACAATTGTCTGCCCCAC

CRISPR/ Cas9 guides were cloned into plasmid pSpCas9(BB)-2A-Puro (PX459) V2.0 (a gift from Feng Zheng, Addgene plasmid #62988; <http://n2t.net/addgene:62988>; RRID:Addgene\_62988) using standard techniques. BV2 cells were nucleofected using a Lonza Nucleofector 2b device (Lonza Bioscience, Morrisville, NC) with Amaxa Kit T nucleofection reagents (Lonza) using program A-030 as instructed by nucleofection manual available on the Lonza website. Cells were allowed to undergo selection and serial dilution produced clonal populations which were then probed for TMEM16F expression by Western blot (TMEM16F antibody, Jan lab) and then sequenced with pGEM®-T Easy Vector cloning (Promega) to determine site of mutation on each strand.

#### *Primary cultures*

Murine microglia cultures were prepared from P3-P5 pups from TMEM16F WT x TMEM16F WT or TMEM16F KO x TMEM16F KO breeding pairs. Three to four cortices per T75 flask was dissected out and minced. Tissue was trypsinized in 0.25% Trypsin EDTA for 25 minutes, shaking once after 10 - 15 minutes. Tissue was washed two times with plating media (Dulbecco's Modified Eagle's Medium (DMEM), high glucose, (Gibco), 10% FBS, 50U/mL PenStrep) and triturated with a 10 mL, 5 mL, and 1 mL pipette. After each trituration step, tissue was allowed to setting and supernatant was passed through a 0.4  $\mu$ m filter. Collected supernatant was spun at 500 x g for 5 minutes and the cell pellet was resuspended and plated into T75 flasks precoated with 100  $\mu$ g/ mL poly-L lysine (PLL). On DIV1, flasks were washed two times with PBS and then plating media plus 10 ng/ml GMCSF (Sigma) was added. On days 7, 12 and 16, flasks were shaken for 3 hours at 37°C at 120 rpm and supernatant (released cells) were plated.

For primary hippocampal and cortical neuronal cultures, cortices and hippocampi were dissected from E15-E18 pups from PS19- TMEM16 WT x PS19+ TMEM16F WT or PS19- TMEM16F KO x PS19+ TMEM16F KO mouse breeding pairs. During dissection, while tissue

from each pup was collected individually in dissection media (HBSS without  $\text{Ca}^{2+}$  and  $\text{Mg}^{2+}$ , 50U/mL PenStrep, 1mM sodium pyruvate, 20mM HEPES, 0.45% glucose), pups were genotyped and samples were pooled based on genotype prior to papain digestion. Dissection media was replaced with dissection media with 200 U/mL papain (that had been heat-activated for at least 30 minutes at 37 °C) for 20 minutes at 37 °C. Papain media was removed and cells were washed with plating media (Dulbecco's Modified Eagle's Medium (DMEM) with high glucose (Gibco), 10% FBS, 50U/mL PenStrep). Neurons were triturated with three to four subsequent flamed glass pipette trituration steps. During each step, after tissue settled, supernatant was passed through a 70  $\mu\text{m}$  filter. Neurons were counted, resuspended in plating media, and plated onto 0.01% poly-L-ornithine (Sigma) coated,  $\text{HNO}_3$ -treated coverslips at a density of 1,300 cells/  $\text{mm}^2$  (150k cells per 12mm glass coverslip or 35mm glass bottom dish). After 30 minutes at 37 °C, plating media was removed and replaced with maintenance media (Neurobasal-Plus, 50U/mL PenStrep, 500  $\mu\text{m}$  Glutamax, 2% B27-Plus ) + 5% horse serum. On DIV1, media was replaced with maintenance media with 0% serum. Twice a week, half of the conditioned media was exchanged for fresh maintenance media.

#### *Extracellular vesicle collection*

Extracellular vesicles were collected through differential ultracentrifugation. Cells were plated in two T75 flasks per genotype and allowed to grow to confluency in DMEM plus 10% FBS (which was spun down at 100,000 x g and filtered 3x through a 0.2 $\mu\text{m}$  filter). Cells were washed twice in calcium-free DPBS and incubated with 3  $\mu\text{M}$  calcium ionophore A23187 (Sigma) in calcium-free DPBS for 5 minutes at 37 °C [47]. Cells were washed once with DPBS and incubated in calcium-containing buffer (140mM NaCl, 2.5mM KCl, 5mM  $\text{CaCl}_2$ , 1.0mM  $\text{MgCl}_2$ , 20mM HEPES, pH7.4) for 1.5 hours at 37 °C. Supernatant was collected from stimulated cells and centrifuged at 200 x g for 5 minutes. Meanwhile, flasks were trypsinized and these cells were added to this pellet obtained from the 500 x g centrifugation. Decanted supernatant

from 500 x g centrifugations was subsequently centrifuged at 2,000 x g for 20 minutes to collect apoptotic bodies and debris. Supernatant was then centrifuged at 16,500 x g for 20 minutes. The resulting supernatant was passed through a 0.2 µm filter and the pellet was resuspended in filtered DPBS and centrifuged once more at 16,500 x g for 20 minutes. This supernatant was passed through a 0.2 µm filter into the collection tube from the first 16,500 x g centrifugation and the MV pellet was collected. Finally, filtered supernatant was centrifuged at 100,000 x g for 60 minutes. Decanted supernatant was discarded and the exosome pellet was collected. All pellets (cell, apoptotic body/ debris, MV, exosome) were kept on ice during the centrifugations and resuspended in 15 µl filtered DPBS for subsequent analyses.

The initial pellet obtained from 500 x g and added trypsinized cells were then counted to establish viability and obtain normalizing values.

### *Biochemistry*

Cell pellets were lysed using RIPA buffer (ThermoFisher). Protein content of resuspended EV pellets and of cells was quantified using Pierce BCA protein assay kit (Thermo Scientific) captured on a Synergy H4 plate reader (BioTek Instruments, Winooski, VT) and SDS sample loading buffer was added to samples. SDS-Page gels were loaded with 20 µg protein per well (or maximum collected EV sample otherwise), run, and then transferred to nitrocellulose membrane using semi-dry transfer with a Trans-Blot Turbo transfer system (Bio-Rad Laboratories, Hercules, CA). After transfer, blots were washed three times quickly with H<sub>2</sub>O, then blocked in 5% milk in TBS + 0.1% Tween 20 (TBST) for 1 hour at room temperature, shaking. After three quick H<sub>2</sub>O washes, blots were incubated in primary antibody in TBST overnight at 4 °C. After primary incubation and three quick H<sub>2</sub>O washes, blots were washed twice with H<sub>2</sub>O for 10 minutes and then one time with TBST for 10 minutes. Antibodies used were TMEM16F developed in the Jan lab (1:2000, rabbit), Alix (1:750, mouse) (Cell Signaling, #2171), and α-tubulin (1:10,000, mouse) (Sigma, #T9026). Washed blots were then incubated

with 1:12,000 secondary HRP anti-rabbit or anti-mouse antibody (Invitrogen) for 1 hour at room temperature, shaking. Finally, they after three quick H<sub>2</sub>O washes, then were washed two times with H<sub>2</sub>O for 10 minutes, one time with TBST for 10 minutes, and then processed with either West Pico or Femto ECL for 3 minutes (Thermo Fisher) and scanned on a C-DiGit Blot Scanner (LI-COR, Lincoln, NE). After development of main protein (TMEM16F or Alix), blots were stripped with stripping buffer (0.2 M glycine, pH 2.5) for 15 minutes and then washed three times with H<sub>2</sub>O. The blot procedure was repeated with the loading control.

### *Nanoparticle Tracking Analysis*

One tenth of resuspended microvesicle or exosome pellets were diluted into 25  $\mu$ l filtered DPBS. Extracellular vesicle concentration (EV/ mL) was determined using nanoparticle tracking analysis (NTA), using a NanoSight LM10 instrument configured with a complementary metal-oxide semiconductor camera and blue 405 nm laser (Mavorn Instruments, Malvern, United Kingdom). Videos were recorded five times for each sample, at 60s each, using a pump flow rate of 40 AU and controlled temperature of 22 °C. All analysis was performed using NTA v3.2 software. Extracellular vesicle counts were normalized to cell counts for data presented.

### *Flow cytometry*

BV2 or primary cells cultured in plating media (DMEM, 10% FBS, 50 U/mL PenStrep) were removed from plates with 0.25% trypsin-EDTA, collected and spun down for 5 minutes at 500 x g. Pellets were washed two times with DPBS with no Ca<sup>2+</sup> or Mg<sup>2+</sup> and counted to 125,000 cells per genotype/tube. Volume was brought to 1 mL with live imaging buffer (140 mM NaCl, 2.5 mM KCl, 5 mM CaCl<sub>2</sub>, 1 mM MgCl<sub>2</sub>, 20 mM HEPES, pH 7.4) and taken to be counted on a FACSCalibur flow cytometer (BD Biosciences, San Jose, CA). Prior to counting, cells were passed up and down and then passed through a 70  $\mu$ M filter. Flow cytometry data was analyzed used FlowJo version 10 software.

### *pHrodo E. Coli plate reader assays*

BV2 or primary cells were seeded into 96 well plates at 75,000 cells per well, 4 replicates per genotype, and left overnight. The next day, cells were washed two times with imaging buffer (DPBS, 20 mM HEPES, 5 mM dextrose, 0.5 M sodium pyruvate). For control cells, 1  $\mu$ M cytochalasin D in imaging buffer and cells were incubated for 10 minutes at 37 °C. *pHrodo E. Coli* was prepared fresh when possible by adding 2 mL to 2 mg pHrodo Red *E. coli* tube (Invitrogen, #P35361). Particles were vortexed for 20 seconds and then sonicated for 1 minute. A 1:5 pHrodo *E. Coli* particles: imaging buffer was added to cells and control no cell wells (100  $\mu$ l per 96 well condition) and taken to a Synergy H4 plate reader and recorded signal every minute for 55 minutes. After recording pHrodo signal, cells were washed two times with buffer. Cells were then incubated with Hoescht 33342 dye (1:500 in imaging buffer, Thermo Scientific, #62249) and 7-AAD viability dye (1:130, BioLegend, # 420403) for 10 minutes at 37 °C and then washed two times with imaging buffer. Signal was read on the Synergy H4 plate reader. Background pHrodo signal from no cell wells was subtracted from other conditions and then these values were normalized to respective Hoescht signal. If 7-AAD signal was high, signal was not included in analysis.

### *pHrodo Red E. Coli and E. Coli 594 live imaging*

Glass bottom 35 mm dishes were pre coated with 100  $\mu$ g/mL PLL and BV2 or primary cells were seeded at 125,000 cells. The next day, *E. Coli* particles were prepared (2 ml imaging buffer into 2 mg particles, plus 2  $\mu$ l of 100x NaN<sub>3</sub> stock (3% w/v). Particles were sonicated for 1 minute. *E. coli* particles were counted using a hemocytometer and added to cells such that there were 30-100 particles per cell. Imaging buffer was supplemented with 1% FBS. For pHrodo particle experiments, particles were added in and plates were imaged on a Nikon-TE2000 Inverted Scope (Nikon Instruments, Melville, NY) with Okolab environmental control incubator cage (37 °C, 5% CO<sub>2</sub>) (Okolab, Ottaviano, Italy) for 1 hour, imaged every 5 minutes. For *E. coli*

594 particles, particles were added into several plates and taken to the microscope, where after every 15 minutes, a plate was quenched with 50  $\mu$ l Trypan blue and imaged. Images were analyzed with ImageJ software.

### *Immunohistochemistry*

Male PS19 TMEM16F mice (either complete knockout or microglial conditional knockout) of various ages (3 month-, 6 month-, 7 month-, 9/10 month-old) were anesthetized using isoflurane and perfused with 1x PBS. Following perfusion, right hemispheres were placed into 4% paraformaldehyde (PFA) in 1x PBS overnight at 4°C. Left hemispheres were frozen on dry ice and stored at -80°C. After fixation, brains were switched into 30% sucrose for two days. Brains were frozen in OCT and sectioned into 40  $\mu$ m thick coronal sections using a Leica CM350 S cryostat (Leica Microsystems, Buffalo Grove, IL). Brain sections were stored cryoprotectant solution (40% 1x PBS, 30% glycerol, 30% ethylene glycol) at -20°C.

### *DAB staining*

Free floating sections were washed eight times in 1x Tris buffered saline (TBS) for 5 minutes. Sections were quenched with 1% hydrogen peroxide ( $H_2O_2$ ) in TBS for 5 minutes and washed three times in TBS for 5 minutes. Blocking was combined with primary incubation in TBS++++ media (1x TBS, 0.13 M glycine, 1.5% bovine serum albumin, 0.4% Triton X-100) at 300  $\mu$ l per 24 well dish for 3 hours, shaking, at room temperature. Either AT8 (1:500, mouse) (a kind gift from Peter Davies) or Iba1 (1:3000, rabbit) (Wako Chemicals, #019-19741) were used. After incubation, sections were washed three times with TBS and incubated with 1:300 secondary HRP anti-mouse or anti-rabbit (Invitrogen) antibody in TBS++++ for 1 hour, shaking, at room temperature. ABC-HRP peroxidase (Vector Laboratories) was prepared, as instructed (1:300 A + 1:300 B) in TBS++++. Sections were washed three times with TBS and replaced with ABC solution for 1 hour, shaking, at room temperature. Afterwards, sections were washed 3

times in 0.1 M Tris pH 8.0 and then stained with DAB for either 1 minute (AT8) or 5 minutes (Iba1), while constantly shaking. Staining was performed in small batches to control time within solution as close as possible to either 1 or 5 minutes, within two or three seconds. DAB solution was prepared fresh before development (0.1 M Tris pH8.0, 1x DAB, 1.5% H<sub>2</sub>O<sub>2</sub>). Finally, sections were washed three times with 0.1 M Tris and mounted onto coverslips and allowed to dry fully overnight. Slides were washed in distilled water (dH<sub>2</sub>O) for 5 minutes, shaking, and then in FD cresyl violet 1:1 solution for 5 minutes. Slides were washed two times in dH<sub>2</sub>O and then went through a series of dehydrations. First, slides were submerged in 95% ethanol (EtOH) with 0.1% glacial acetic acid for 15 seconds, then incubated in two 100% EtOH washes for 2 minutes each. Slides were then incubated two times in xylene for 5 minutes each and finally coverslipped using Permount mounting media (Fisher). After drying, sections were imaged using an Aperio AT2 slide scanner (Leica Biosystems, Buffalo Grove, IL). Images were processed and analyzed with Slide Scope Virtual Scan and ImageJ software.

### *Immunocytochemistry*

Cells on coverslips were washed three times with PBS for 5 minutes and then fixed for 8 minutes at room temperature with 4% PFA in PBS. Cells were washed 3 times with TBS and incubated in blocking/ primary solution TBS++++ for 3 hours at room temperature or overnight at 4 °C. Map2 (1:100, rb) (Chemicon, #AB5622), AT8 (1:500, ms), and CD11b-FITC (1:100) (eBioscience, # 53-0112) were used. Cells were washed two times with TBS for 5 minutes and two times with TBSTx (TBS, 0.1% Triton X-100) for 10 minutes. Coverslips were then incubated for 1 hour with secondary 1:500 Alexa 555 or Alexa 647 anti- mouse or rabbit (Invitrogen). They were washed two times with TBS for 5 minutes and two times with TBSTx for 10 minutes. Coverslips were finally mounted onto coverslips using DAPI FluorMount-G (SouthernBiotech). Once dry, coverslips were imaged using an SP8-X inverted confocal microscope with HyD hybrid detectors (Leica Microsystems, Wetzlar, Germany).



### *PS exposure assay*

On DIV 16-18, cultured primary neurons were washed twice with DPBS and then incubated with 2  $\mu$ M NeuroFluor NeuO (Stem Cell Technologies, #01801) in neuronal maintenance media for 1 hour at 37 °C. Neurons were washed two times with maintenance media and left until stained or three times with physiological saline solution (140 mM NaCl, 4 mM KCl, 2.5 mM CaCl<sub>2</sub>, 1 mM MgCl<sub>2</sub>, 10 mM dextrose, 10 mM HEPES, 0.1 mM EGTA, pH 7.4) (PSS) if was about to be processed. Neurons were incubated in Annexin V APC (1:200) (BD Biosciences, #550474) and NuvView (1:200) (Biotium, #10405) for 15 minutes at 37 °C. Neurons were washed three times with PSS and then imaged using a Leica SP8-X inverted confocal microscope with HyD hybrid detectors, adaptive focus control, and Okolab environmental control incubator cage (37 °C, 5% CO<sub>2</sub>). 40-45 areas of the coverslip were selected based on NeuroFluor NeuO and then imaged.

### *Behavioral Assays*

Male PS19 Cx3cr1-Cre mice 28-32 weeks of age were transferred to the Gladstone Behavioral Core and acclimated to the new housing at least 2 weeks prior to any testing. Researchers conducting all behavioral tests were blinded to the mouse genotype during testing and analysis. Statistical analysis for all behavioral tests was completed using Prism 7 (GraphPad, RRID:SCR\_002798).

### *Elevated Plus Maze*

Mice were brought into the testing room to acclimate in dim light 1 hour prior to testing. Mice were placed in the center of an elevated plus maze (Kinder Scientific Inc., Poway, CA) at the start of testing and allowed to freely explore the maze for 10 minutes. The elevated plus maze was situated 63 cm above the ground and was comprised of two “closed” arms (38 x 5 x 5 cm) with high walls (16.5 cm) and two “open” arms (38 x 5 x 5 cm) without any walls. The software

recorded time and distance traveled as well as the entries into each arm using infrared photobeam breaks. The maze was cleaned with 70% ethanol between mice.

### *Open Field*

Mice were brought into the testing room to acclimate 1 hour prior to testing in normal light. Mice were placed in the middle of clear acrylic enclosures (41 x 41 x 30 cm) that were housed inside larger sound and light attenuating cubicles (Lafayette Instruments, Lafayette, IN). All mice were allowed to freely explore the enclosure for 15 minutes. The Flex-field/Open Field Photobeam Activity System (San Diego Instruments Inc., San Diego, CA) was used to track ambulatory and fine movements as well as rearing behavior using infrared photobeam arrays placed just outside the enclosure. The box was cleaned with 70% ethanol between mice.

### *Interactive Place Avoidance*

Mice were transferred to testing room 60 minutes prior to testing to habituate and acclimate. Testing was performed using the BioSignal Corp. Place Avoidance system and Tracker software. Distinct black & white visual cues were placed on the walls of the room surrounding the apparatus [173]. The mice were placed inside a plexiglass cylinder (40 cm diameter) with a lid and the cylinder and grid were cleaned with 70% alcohol between trials. 30 animals can be tested per group, per week (five to six trials). Trials were 10 minutes in length and each animal was given one trial per day. The Probe/Reinstatement test on Day 5 was split into two 5 min segments, with the Probe segment first with the current source (shock) turned off while the Reinstatement segment occurs during the second 5 minutes with the current source being turned back on but not until the mouse completely left the shock zone if still present after the first 5 minutes. The grid arena was rotated at 1 RPM clockwise during the trials such that the animal must actively navigate against the rotation of the arena otherwise they entered the aversive zone (circle, box or wedge of space designated by the experimenter as the aversive

zone which was fixed relative to the external configuration of spatial cues surrounding the arena (Active Avoidance). The Tracker program video tracked the animal's path within the arena. When the animal entered the aversive zone, the Tracker activated a 0.2 mA current source for 500 milliseconds and issued it repeatedly every 1.5 seconds until the animal left the zone.

### *Hot Plate Test*

Mice were transferred to testing room 60 minutes prior to testing to habituate and acclimate. The hot plate test was measured on a black anodized, aluminum plate (IITC Life Science Inc., Woodland Hills, CA) which is heated to a constant temperature of 52°C, as measured by a built-in digital thermometer. During testing, mice were placed in clear, open-ended cylindrical enclosure, which was placed on top of the hot plate. The latency to respond with either a hind paw lick, hind paw flick, or jump (whichever comes first) was measured and the experimenter stopped the timer when the response was observed. The mouse was immediately removed from the hot plate and returned to its home cage. Each animal was only tested once and to prevent injury, the maximum latency was 30 seconds. The hot plate was cleaned with 70% ethanol between mice.

## 5.1 FIGURES

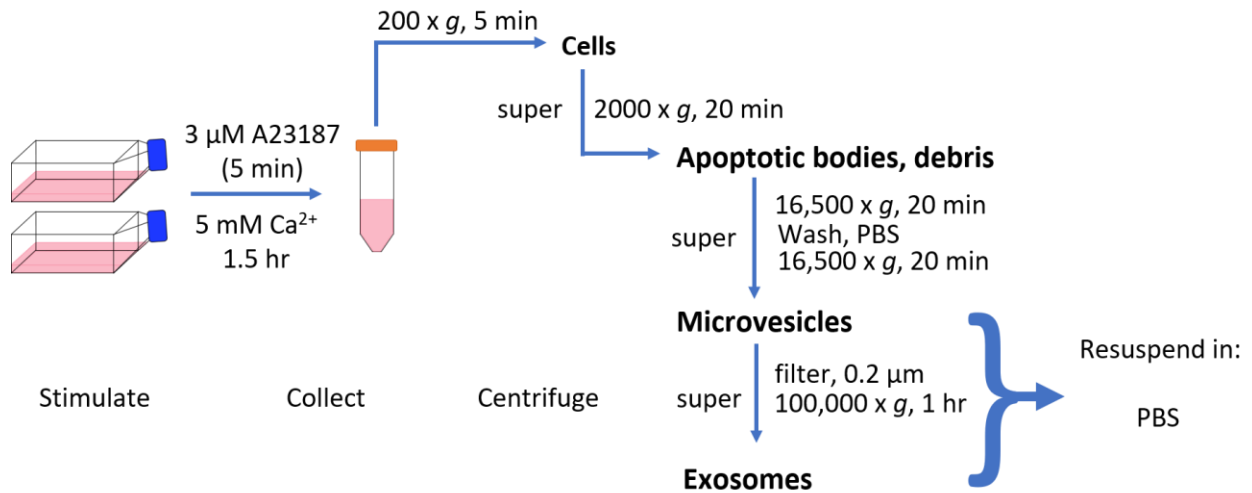


**Figure 5.1 Schematic of extracellular vesicle collection.** Full detail is listed under “*Extracellular vesicle collection*”, but briefly cells were stimulated with  $\text{Ca}^{2+}$  ionophore A23187 and then supernatant was collected. After each centrifugation step of increased speed, the pellet was collected, and the supernatant was used for subsequent centrifugations.

## REFERENCES

- [1] M. Katoh and M. Katoh, "FLJ10261 gene, located within the CCND1-EMS1 locus on human chromosome 11q13, encodes the eight-transmembrane protein homologous to C12orf3, C11orf25 and FLJ34272 gene products," *Int J Oncol*, vol. 22, pp. 1375-81, Jun 2003.
- [2] J. Suzuki, M. Umeda, P. J. Sims, and S. Nagata, "Calcium-dependent phospholipid scrambling by TMEM16F," *Nature*, vol. 468, pp. 834-8, Dec 9 2010.
- [3] J. Ousingsawat, P. Wanitchakool, A. Kmit, A. M. Romao, W. Jantarajit, R. Schreiber, *et al.*, "Anoctamin 6 mediates effects essential for innate immunity downstream of P2X7 receptors in macrophages," *Nat Commun*, vol. 6, p. 6245, 2015.
- [4] N. Pedemonte and L. J. Galletta, "Structure and function of TMEM16 proteins (anoctamins)," *Physiol Rev*, vol. 94, pp. 419-59, Apr 2014.
- [5] A. Picollo, M. Malvezzi, and A. Accardi, "TMEM16 proteins: unknown structure and confusing functions," *J Mol Biol*, vol. 427, pp. 94-105, Jan 16 2015.
- [6] J. M. Whitlock and H. C. Hartzell, "Anoctamins/TMEM16 Proteins: Chloride Channels Flirting with Lipids and Extracellular Vesicles," *Annu Rev Physiol*, vol. 79, pp. 119-143, Feb 10 2017.
- [7] H. Yang, A. Kim, T. David, D. Palmer, T. Jin, J. Tien, *et al.*, "TMEM16F forms a Ca<sup>2+</sup>-activated cation channel required for lipid scrambling in platelets during blood coagulation," *Cell*, vol. 151, pp. 111-22, Sep 28 2012.
- [8] C. Duran and H. C. Hartzell, "Physiological roles and diseases of Tmem16/Anoctamin proteins: are they all chloride channels?," *Acta Pharmacol Sin*, vol. 32, pp. 685-92, Jun 2011.
- [9] C. Hartzell, I. Putzier, and J. Arreola, "Calcium-activated chloride channels," *Annu Rev Physiol*, vol. 67, pp. 719-58, 2005.

- [10] A. Caputo, E. Caci, L. Ferrera, N. Pedemonte, C. Barsanti, E. Sondo, *et al.*, "TMEM16A, a membrane protein associated with calcium-dependent chloride channel activity," *Science*, vol. 322, pp. 590-4, Oct 24 2008.
- [11] B. C. Schroeder, T. Cheng, Y. N. Jan, and L. Y. Jan, "Expression cloning of TMEM16A as a calcium-activated chloride channel subunit," *Cell*, vol. 134, pp. 1019-29, Sep 19 2008.
- [12] Y. D. Yang, H. Cho, J. Y. Koo, M. H. Tak, Y. Cho, W. S. Shim, *et al.*, "TMEM16A confers receptor-activated calcium-dependent chloride conductance," *Nature*, vol. 455, pp. 1210-5, Oct 30 2008.
- [13] M. He, W. Ye, W. J. Wang, E. S. Sison, Y. N. Jan, and L. Y. Jan, "Cytoplasmic Cl<sup>(-)</sup> couples membrane remodeling to epithelial morphogenesis," *Proc Natl Acad Sci U S A*, vol. 114, pp. E11161-e11169, Dec 26 2017.
- [14] B. Ayoglu, N. Mitsios, I. Kockum, M. Khademi, A. Zandian, R. Sjöberg, *et al.*, "Anoctamin 2 identified as an autoimmune target in multiple sclerosis," *Proc Natl Acad Sci U S A*, vol. 113, pp. 2188-93, Feb 23 2016.
- [15] D. Crottès and L. Y. Jan, "The multifaceted role of TMEM16A in cancer," *Cell Calcium*, vol. 82, p. 102050, Sep 2019.
- [16] X. M. Wong, S. Younger, C. J. Peters, Y. N. Jan, and L. Y. Jan, "Subdued, a TMEM16 family Ca<sup>2+</sup>-activated Cl<sup>-</sup> channel in *Drosophila melanogaster* with an unexpected role in host defense," *Elife*, vol. 2, p. e00862, Nov 5 2013.
- [17] M. E. Falzone, M. Malvezzi, B. C. Lee, and A. Accardi, "Known structures and unknown mechanisms of TMEM16 scramblases and channels," *J Gen Physiol*, vol. 150, pp. 933-947, Jul 2 2018.
- [18] M. Malvezzi, M. Chalal, R. Janjusevic, A. Picollo, H. Terashima, A. K. Menon, *et al.*, "Ca<sup>2+</sup>-dependent phospholipid scrambling by a reconstituted TMEM16 ion channel," *Nat Commun*, vol. 4, p. 2367, 2013.

- [19] B. C. Lee, A. K. Menon, and A. Accardi, "The nhTMEM16 Scramblase Is Also a Nonselective Ion Channel," *Biophys J*, vol. 111, pp. 1919-1924, Nov 1 2016.
- [20] L. Wang, "Functional Studies of the TMEM16B Calcium-activated Chloride Channel in the Lateral Septum," Neuroscience Dept., UCSF, 2018.
- [21] L. Wang, J. Simms, C. J. Peters, M. Tynan-La Fontaine, K. Li, T. M. Gill, *et al.*, "TMEM16B Calcium-Activated Chloride Channels Regulate Action Potential Firing in Lateral Septum and Aggression in Male Mice," *J Neurosci*, vol. 39, pp. 7102-7117, Sep 4 2019.
- [22] F. Huang, X. Wang, E. M. Ostertag, T. Nuwal, B. Huang, Y. N. Jan, *et al.*, "TMEM16C facilitates Na(+)-activated K<sup>+</sup> currents in rat sensory neurons and regulates pain processing," *Nat Neurosci*, vol. 16, pp. 1284-90, Sep 2013.
- [23] V. Bolduc, G. Marlow, K. M. Boycott, K. Saleki, H. Inoue, J. Kroon, *et al.*, "Recessive mutations in the putative calcium-activated chloride channel Anoctamin 5 cause proximal LGMD2L and distal MMD3 muscular dystrophies," *Am J Hum Genet*, vol. 86, pp. 213-21, Feb 12 2010.
- [24] K. Mizuta, S. Tsutsumi, H. Inoue, Y. Sakamoto, K. Miyatake, K. Miyawaki, *et al.*, "Molecular characterization of GDD1/TMEM16E, the gene product responsible for autosomal dominant gnathodiaphyseal dysplasia," *Biochem Biophys Res Commun*, vol. 357, pp. 126-32, May 25 2007.
- [25] S. Tsutsumi, N. Kamata, T. J. Vokes, Y. Maruoka, K. Nakakuki, S. Enomoto, *et al.*, "The novel gene encoding a putative transmembrane protein is mutated in gnathodiaphyseal dysplasia (GDD)," *Am J Hum Genet*, vol. 74, pp. 1255-61, Jun 2004.
- [26] C. Bricogne, M. Fine, P. M. Pereira, J. Sung, M. Tijani, Y. Wang, *et al.*, "TMEM16F activation by Ca(2+) triggers plasma membrane expansion and directs PD-1 trafficking," *Sci Rep*, vol. 9, p. 619, Jan 24 2019.



- [27] T. Fujii, A. Sakata, S. Nishimura, K. Eto, and S. Nagata, "TMEM16F is required for phosphatidylserine exposure and microparticle release in activated mouse platelets," *Proceedings of the National Academy of Sciences*, vol. 112, p. 12800, 2015.
- [28] L. K. Schenk, J. Ousingsawat, B. V. Skryabin, R. Schreiber, H. Pavenstädt, and K. Kunzelmann, "Regulation and Function of TMEM16F in Renal Podocytes," *Int J Mol Sci*, vol. 19, Jun 18 2018.
- [29] Y. Hu, J. H. Kim, K. He, Q. Wan, J. Kim, M. Flach, *et al.*, "Scramblase TMEM16F terminates T cell receptor signaling to restrict T cell exhaustion," *J Exp Med*, vol. 213, pp. 2759-2772, Nov 14 2016.
- [30] S. Das, Y. Hahn, S. Nagata, M. C. Willingham, T. K. Bera, B. Lee, *et al.*, "NGEP, a prostate-specific plasma membrane protein that promotes the association of LNCaP cells," *Cancer Res*, vol. 67, pp. 1594-601, Feb 15 2007.
- [31] M. Petkovic, J. Osés-Prieto, A. Burlingame, L. Y. Jan, and Y. N. Jan, "TMEM16K is an interorganelle regulator of endosomal sorting," *Nat Commun*, vol. 11, p. 3298, Jul 3 2020.
- [32] S. Gyobu, K. Ishihara, J. Suzuki, K. Segawa, and S. Nagata, "Characterization of the scrambling domain of the TMEM16 family," *Proc Natl Acad Sci U S A*, vol. 114, pp. 6274-6279, Jun 13 2017.
- [33] J. Suzuki, T. Fujii, T. Imao, K. Ishihara, H. Kuba, and S. Nagata, "Calcium-dependent phospholipid scramblase activity of TMEM16 protein family members," *J Biol Chem*, vol. 288, pp. 13305-16, May 10 2013.
- [34] D. L. Daleke, "Regulation of transbilayer plasma membrane phospholipid asymmetry," *Lipid Res*, vol. 44, pp. 233-42, Feb 2003.
- [35] P. A. Leventis and S. Grinstein, "The distribution and function of phosphatidylserine in cellular membranes," *Annu Rev Biophys*, vol. 39, pp. 407-27, 2010.

- [36] G. van Meer, D. R. Voelker, and G. W. Feigenson, "Membrane lipids: where they are and how they behave," *Nature reviews. Molecular cell biology*, vol. 9, pp. 112-124, 2008.
- [37] E. M. Bevers and P. L. Williamson, "Phospholipid scramblase: an update," *FEBS Lett*, vol. 584, pp. 2724-30, Jul 2 2010.
- [38] G. van Meer, "Dynamic transbilayer lipid asymmetry," *Cold Spring Harb Perspect Biol*, vol. 3, May 1 2011.
- [39] R. F. Zwaal, P. Comfurius, and E. M. Bevers, "Scott syndrome, a bleeding disorder caused by defective scrambling of membrane phospholipids," *Biochim Biophys Acta*, vol. 1636, pp. 119-28, Mar 22 2004.
- [40] F. Bassé, J. G. Stout, P. J. Sims, and T. Wiedmer, "Isolation of an erythrocyte membrane protein that mediates Ca<sup>2+</sup>-dependent transbilayer movement of phospholipid," *J Biol Chem*, vol. 271, pp. 17205-10, Jul 19 1996.
- [41] Q. Zhou, J. Zhao, J. G. Stout, R. A. Luhm, T. Wiedmer, and P. J. Sims, "Molecular cloning of human plasma membrane phospholipid scramblase. A protein mediating transbilayer movement of plasma membrane phospholipids," *J Biol Chem*, vol. 272, pp. 18240-4, Jul 18 1997.
- [42] S. K. Sahu, S. N. Gummadi, N. Manoj, and G. K. Aradhyam, "Phospholipid scramblases: an overview," *Arch Biochem Biophys*, vol. 462, pp. 103-14, Jun 1 2007.
- [43] E. Castoldi, P. W. Collins, P. L. Williamson, and E. M. Bevers, "Compound heterozygosity for 2 novel TMEM16F mutations in a patient with Scott syndrome," *Blood*, vol. 117, pp. 4399-400, Apr 21 2011.
- [44] J. D. Brunner, N. K. Lim, S. Schenck, A. Duerst, and R. Dutzler, "X-ray structure of a calcium-activated TMEM16 lipid scramblase," *Nature*, vol. 516, pp. 207-12, Dec 11 2014.

- [45] S. Dang, S. Feng, J. Tien, C. J. Peters, D. Bulkley, M. Lolicato, *et al.*, "Cryo-EM structures of the TMEM16A calcium-activated chloride channel," *Nature*, vol. 552, pp. 426-429, Dec 21 2017.
- [46] C. Paulino, V. Kalienkova, A. K. M. Lam, Y. Neldner, and R. Dutzler, "Activation mechanism of the calcium-activated chloride channel TMEM16A revealed by cryo-EM," *Nature*, vol. 552, pp. 421-425, Dec 21 2017.
- [47] K. Yu, J. M. Whitlock, K. Lee, E. A. Ortlund, Y. Y. Cui, and H. C. Hartzell, "Identification of a lipid scrambling domain in ANO6/TMEM16F," *Elife*, vol. 4, p. e06901, 2015.
- [48] T. Suzuki, J. Suzuki, and S. Nagata, "Functional swapping between transmembrane proteins TMEM16A and TMEM16F," *J Biol Chem*, vol. 289, pp. 7438-47, Mar 14 2014.
- [49] S. Feng, S. Dang, T. W. Han, W. Ye, P. Jin, T. Cheng, *et al.*, "Cryo-EM Studies of TMEM16F Calcium-Activated Ion Channel Suggest Features Important for Lipid Scrambling," *Cell Rep*, vol. 28, pp. 567-579.e4, Jul 9 2019.
- [50] V. Kalienkova, V. Clerico Mosina, L. Bryner, G. T. Oostergetel, R. Dutzler, and C. Paulino, "Stepwise activation mechanism of the scramblase nhTMEM16 revealed by cryo-EM," *Elife*, vol. 8, Feb 21 2019.
- [51] G. Khelashvili, M. E. Falzone, X. Cheng, B. C. Lee, A. Accardi, and H. Weinstein, "Dynamic modulation of the lipid translocation groove generates a conductive ion channel in Ca(2+)-bound nhTMEM16," *Nat Commun*, vol. 10, p. 4972, Oct 31 2019.
- [52] C. Paulino, Y. Neldner, A. K. Lam, V. Kalienkova, J. D. Brunner, S. Schenck, *et al.*, "Structural basis for anion conduction in the calcium-activated chloride channel TMEM16A," *Elife*, vol. 6, May 31 2017.
- [53] F. Bleibaum, A. Sommer, M. Veit, B. Rabe, J. Andrä, K. Kunzelmann, *et al.*, "ADAM10 sheddase activation is controlled by cell membrane asymmetry," *J Mol Cell Biol*, vol. 11, pp. 979-993, Dec 23 2019.

- [54] Y. Hu, J. H. Kim, K. He, Q. Wan, J. Kim, M. Flach, *et al.*, "Scramblase TMEM16F terminates T cell receptor signaling to restrict T cell exhaustion," *Journal of Experimental Medicine*, vol. 213, pp. 2759-2772, 2016.
- [55] E. Zaitseva, E. Zaitsev, K. Melikov, A. Arakelyan, M. Marin, R. Villasmil, *et al.*, "Fusion Stage of HIV-1 Entry Depends on Virus-Induced Cell Surface Exposure of Phosphatidylserine," *Cell Host Microbe*, vol. 22, pp. 99-110.e7, Jul 12 2017.
- [56] B. A. Chua, J. A. Ngo, K. Situ, and K. Morizono, "Roles of phosphatidylserine exposed on the viral envelope and cell membrane in HIV-1 replication," *Cell Commun Signal*, vol. 17, p. 132, Oct 21 2019.
- [57] P. Younan, M. Iampietro, R. I. Santos, P. Ramanathan, V. L. Popov, and A. Bukreyev, "Role of Transmembrane Protein 16F in the Incorporation of Phosphatidylserine Into Budding Ebola Virus Virions," *J Infect Dis*, vol. 218, pp. S335-s345, Nov 22 2018.
- [58] N. Wu, V. Cernysiov, D. Davidson, H. Song, J. Tang, S. Luo, *et al.*, "Critical Role of Lipid Scramblase TMEM16F in Phosphatidylserine Exposure and Repair of Plasma Membrane after Pore Formation," *Cell Rep*, vol. 30, pp. 1129-1140.e5, Jan 28 2020.
- [59] S. E. Headland, H. R. Jones, L. V. Norling, A. Kim, P. R. Souza, E. Corsiero, *et al.*, "Neutrophil-derived microvesicles enter cartilage and protect the joint in inflammatory arthritis," *Sci Transl Med*, vol. 7, p. 315ra190, Nov 25 2015.
- [60] H. W. Ehlen, M. Chinenkova, M. Moser, H. M. Munter, Y. Krause, S. Gross, *et al.*, "Inactivation of anoctamin-6/Tmem16f, a regulator of phosphatidylserine scrambling in osteoblasts, leads to decreased mineral deposition in skeletal tissues," *J Bone Miner Res*, vol. 28, pp. 246-59, Feb 2013.
- [61] C. Soulard, C. Salsac, K. Mouzat, C. Hilaire, J. Roussel, A. Mezghrani, *et al.*, "Spinal Motoneuron TMEM16F Acts at C-boutons to Modulate Motor Resistance and Contributes to ALS Pathogenesis," *Cell Reports*, vol. 30, pp. 2581-2593.e7, 2020/02/25/2020.

- [62] L. Batti, M. Sundukova, E. Murana, S. Pimpinella, F. De Castro Reis, F. Pagani, *et al.*, "TMEM16F Regulates Spinal Microglial Function in Neuropathic Pain States," *Cell Reports*, vol. 15, pp. 2608-2615, 2016.
- [63] J. Zhao and Q. Y. Gao, "TMEM16F inhibition limits pain-associated behavior and improves motor function by promoting microglia M2 polarization in mice," *Biochem Biophys Res Commun*, vol. 517, pp. 603-610, Oct 1 2019.
- [64] Y. Zhang, H. Li, X. Li, J. Wu, T. Xue, J. Wu, *et al.*, "TMEM16F Aggravates Neuronal Loss by Mediating Microglial Phagocytosis of Neurons in a Rat Experimental Cerebral Ischemia and Reperfusion Model," *Frontiers in Immunology*, vol. 11, p. 1144, 2020.
- [65] G. W. Gould and J. Lippincott-Schwartz, "New roles for endosomes: from vesicular carriers to multi-purpose platforms," *Nat Rev Mol Cell Biol*, vol. 10, pp. 287-92, Apr 2009.
- [66] C. Thery, L. Zitvogel, and S. Amigorena, "Exosomes: composition, biogenesis and function," *Nat Rev Immunol*, vol. 2, pp. 569-79, Aug 2002.
- [67] M. Colombo, C. Moita, G. van Niel, J. Kowal, J. Vigneron, P. Benaroch, *et al.*, "Analysis of ESCRT functions in exosome biogenesis, composition and secretion highlights the heterogeneity of extracellular vesicles," *J Cell Sci*, vol. 126, pp. 5553-65, Dec 15 2013.
- [68] J. De Toro, L. Herschlik, C. Waldner, and C. Mongini, "Emerging roles of exosomes in normal and pathological conditions: new insights for diagnosis and therapeutic applications," *Front Immunol*, vol. 6, p. 203, 2015.
- [69] B. Gyorgy, T. G. Szabo, M. Pasztoi, Z. Pal, P. Misjak, B. Aradi, *et al.*, "Membrane vesicles, current state-of-the-art: emerging role of extracellular vesicles," *Cell Mol Life Sci*, vol. 68, pp. 2667-88, Aug 2011.
- [70] M. Tkach and C. Thery, "Communication by Extracellular Vesicles: Where We Are and Where We Need to Go," *Cell*, vol. 164, pp. 1226-32, Mar 10 2016.
- [71] E. Cocucci and J. Meldolesi, "Ectosomes and exosomes: shedding the confusion between extracellular vesicles," *Trends Cell Biol*, vol. 25, pp. 364-72, Jun 2015.

- [72] M. Colombo, G. Raposo, and C. Thery, "Biogenesis, secretion, and intercellular interactions of exosomes and other extracellular vesicles," *Annu Rev Cell Dev Biol*, vol. 30, pp. 255-89, 2014.
- [73] P. I. Hanson and A. Cashikar, "Multivesicular body morphogenesis," *Annu Rev Cell Dev Biol*, vol. 28, pp. 337-62, 2012.
- [74] W. M. Henne, N. J. Buchkovich, and S. D. Emr, "The ESCRT pathway," *Dev Cell*, vol. 21, pp. 77-91, Jul 19 2011.
- [75] I. Roxrud, H. Stenmark, and L. Malerød, "ESCRT & Co," *Biol Cell*, vol. 102, pp. 293-318, Mar 12 2010.
- [76] J. H. Hurley and P. I. Hanson, "Membrane budding and scission by the ESCRT machinery: it's all in the neck," *Nat Rev Mol Cell Biol*, vol. 11, pp. 556-66, Aug 2010.
- [77] T. Wollert, C. Wunder, J. Lippincott-Schwartz, and J. H. Hurley, "Membrane scission by the ESCRT-III complex," *Nature*, vol. 458, pp. 172-7, Mar 12 2009.
- [78] G. van Niel, G. D'Angelo, and G. Raposo, "Shedding light on the cell biology of extracellular vesicles," *Nature Reviews Molecular Cell Biology*, vol. 19, pp. 213-228, 2018/04/01 2018.
- [79] H. Valadi, K. Ekström, A. Bossios, M. Sjöstrand, J. J. Lee, and J. O. Lötvall, "Exosome-mediated transfer of mRNAs and microRNAs is a novel mechanism of genetic exchange between cells," *Nature Cell Biology*, vol. 9, pp. 654-659, 2007/06/01 2007.
- [80] I. Prada and J. Meldolesi, "Binding and Fusion of Extracellular Vesicles to the Plasma Membrane of Their Cell Targets," *International Journal of Molecular Sciences*, vol. 17, 2016.
- [81] A. Montecalvo, A. T. Larregina, W. J. Shufesky, D. Beer Stolz, M. L. G. Sullivan, J. M. Karlsson, *et al.*, "Mechanism of transfer of functional microRNAs between mouse dendritic cells via exosomes," *Blood*, vol. 119, pp. 756-766, 2012.

- [82] A. Chairoungdua, D. L. Smith, P. Pochard, M. Hull, and M. J. Caplan, "Exosome release of  $\beta$ -catenin: a novel mechanism that antagonizes Wnt signaling," *Journal of Cell Biology*, vol. 190, pp. 1079-1091, 2010.
- [83] G. Raposo and W. Stoorvogel, "Extracellular vesicles: exosomes, microvesicles, and friends," *J Cell Biol*, vol. 200, pp. 373-83, Feb 18 2013.
- [84] R. Kalluri and V. S. LeBleu, "Discovery of Double-Stranded Genomic DNA in Circulating Exosomes," *Cold Spring Harb Symp Quant Biol*, vol. 81, pp. 275-280, 2016.
- [85] W. C. Newton, J. W. Kim, J. Z. Q. Luo, and L. Luo, "Stem cell-derived exosomes: a novel vector for tissue repair and diabetic therapy," *Journal of Molecular Endocrinology*, vol. 59, pp. R155-R165, 01 Nov. 2017 2017.
- [86] V. Budnik, C. Ruiz-Canada, and F. Wendler, "Extracellular vesicles round off communication in the nervous system," *Nat Rev Neurosci*, vol. 17, pp. 160-72, Mar 2016.
- [87] L. Morel, M. Regan, H. Higashimori, S. K. Ng, C. Esau, S. Vidensky, *et al.*, "Neuronal exosomal miRNA-dependent translational regulation of astroglial glutamate transporter GLT1," *J Biol Chem*, vol. 288, pp. 7105-16, Mar 8 2013.
- [88] C. Frühbeis, D. Fröhlich, W. P. Kuo, J. Amphornrat, S. Thilemann, A. S. Saab, *et al.*, "Neurotransmitter-triggered transfer of exosomes mediates oligodendrocyte-neuron communication," *PLoS Biol*, vol. 11, p. e1001604, Jul 2013.
- [89] D. Fröhlich, W. P. Kuo, C. Frühbeis, J. J. Sun, C. M. Zehendner, H. J. Luhmann, *et al.*, "Multifaceted effects of oligodendroglial exosomes on neurons: impact on neuronal firing rate, signal transduction and gene regulation," *Philos Trans R Soc Lond B Biol Sci*, vol. 369, Sep 26 2014.
- [90] M. Bakhti, C. Winter, and M. Simons, "Inhibition of myelin membrane sheath formation by oligodendrocyte-derived exosome-like vesicles," *J Biol Chem*, vol. 286, pp. 787-96, Jan 7 2011.

- [91] F. Antonucci, E. Turola, L. Riganti, M. Caleo, M. Gabrielli, C. Perrotta, *et al.*, "Microvesicles released from microglia stimulate synaptic activity via enhanced sphingolipid metabolism," *Embo j*, vol. 31, pp. 1231-40, Mar 7 2012.
- [92] M. Gabrielli, N. Battista, L. Riganti, I. Prada, F. Antonucci, L. Cantone, *et al.*, "Active endocannabinoids are secreted on extracellular membrane vesicles," *EMBO Rep*, vol. 16, pp. 213-20, Feb 2015.
- [93] I. Potolicchio, G. J. Carven, X. Xu, C. Stipp, R. J. Riese, L. J. Stern, *et al.*, "Proteomic analysis of microglia-derived exosomes: metabolic role of the aminopeptidase CD13 in neuropeptide catabolism," *J Immunol*, vol. 175, pp. 2237-43, Aug 15 2005.
- [94] K. Glebov, M. Löchner, R. Jabs, T. Lau, O. Merkel, P. Schloss, *et al.*, "Serotonin stimulates secretion of exosomes from microglia cells," *Glia*, vol. 63, pp. 626-34, Apr 2015.
- [95] F. Bianco, C. Perrotta, L. Novellino, M. Francolini, L. Riganti, E. Menna, *et al.*, "Acid sphingomyelinase activity triggers microparticle release from glial cells," *Embo j*, vol. 28, pp. 1043-54, Apr 22 2009.
- [96] F. Bianco, E. Pravettoni, A. Colombo, U. Schenk, T. Moller, M. Matteoli, *et al.*, "Astrocyte-Derived ATP Induces Vesicle Shedding and IL-1 Release from Microglia," *The Journal of Immunology*, vol. 174, pp. 7268-7277, 2005.
- [97] S. Wang, F. Cesca, G. Loers, M. Schweizer, F. Buck, F. Benfenati, *et al.*, "Synapsin I is an oligomannose-carrying glycoprotein, acts as an oligomannose-binding lectin, and promotes neurite outgrowth and neuronal survival when released via glia-derived exosomes," *J Neurosci*, vol. 31, pp. 7275-90, May 18 2011.
- [98] A. Hoshino, B. Costa-Silva, T. L. Shen, G. Rodrigues, A. Hashimoto, M. Tesic Mark, *et al.*, "Tumour exosome integrins determine organotropic metastasis," *Nature*, vol. 527, pp. 329-35, Nov 19 2015.



- [99] A. P. Owens, 3rd and N. Mackman, "Microparticles in hemostasis and thrombosis," *Circ Res*, vol. 108, pp. 1284-97, May 13 2011.
- [100] M. Vanwijk, E. Vanbavel, A. Sturk, and R. Nieuwland, "Microparticles in cardiovascular diseases," *Cardiovascular Research*, vol. 59, pp. 277-287, 2003.
- [101] E. Boilard, P. A. Nigrovic, K. Larabee, G. F. Watts, J. S. Coblyn, M. E. Weinblatt, *et al.*, "Platelets amplify inflammation in arthritis via collagen-dependent microparticle production," *Science*, vol. 327, pp. 580-3, Jan 29 2010.
- [102] T. H. Lee, E. D'Asti, N. Magnus, K. Al-Nedawi, B. Meehan, and J. Rak, "Microvesicles as mediators of intercellular communication in cancer--the emerging science of cellular 'debris'," *Semin Immunopathol*, vol. 33, pp. 455-67, Sep 2011.
- [103] P. Joshi, E. Turola, A. Ruiz, A. Bergami, D. D. Libera, L. Benussi, *et al.*, "Microglia convert aggregated amyloid-beta into neurotoxic forms through the shedding of microvesicles," *Cell Death Differ*, vol. 21, pp. 582-93, Apr 2014.
- [104] C. Chang, H. Lang, N. Geng, J. Wang, N. Li, and X. Wang, "Exosomes of BV-2 cells induced by alpha-synuclein: important mediator of neurodegeneration in PD," *Neurosci Lett*, vol. 548, pp. 190-5, Aug 26 2013.
- [105] S. Dujardin, S. Begard, R. Caillierez, C. Lachaud, L. Delattre, S. Carrier, *et al.*, "Ectosomes: a new mechanism for non-exosomal secretion of tau protein," *PLoS One*, vol. 9, p. e100760, 2014.
- [106] J. C. Polanco, B. J. Scicluna, A. F. Hill, and J. Gotz, "Extracellular Vesicles Isolated from the Brains of rTg4510 Mice Seed Tau Protein Aggregation in a Threshold-dependent Manner," *J Biol Chem*, vol. 291, pp. 12445-66, Jun 10 2016.
- [107] H. Asai, S. Ikezu, S. Tsunoda, M. Medalla, J. Luebke, T. Haydar, *et al.*, "Depletion of microglia and inhibition of exosome synthesis halt tau propagation," *Nat Neurosci*, vol. 18, pp. 1584-93, Nov 2015.

- [108] L. Alvarez-Erviti, Y. Seow, A. H. Schapira, C. Gardiner, I. L. Sargent, M. J. Wood, *et al.*, "Lysosomal dysfunction increases exosome-mediated alpha-synuclein release and transmission," *Neurobiol Dis*, vol. 42, pp. 360-7, Jun 2011.
- [109] "2020 Alzheimer's disease facts and figures," *Alzheimers Dement*, Mar 10 2020.
- [110] S. Jäkel and L. Dimou, "Glial Cells and Their Function in the Adult Brain: A Journey through the History of Their Ablation," *Frontiers in Cellular Neuroscience*, vol. 11, 2017-February-13 2017.
- [111] M. G. Erkinen, M.-O. Kim, and M. D. Geschwind, "Clinical Neurology and Epidemiology of the Major Neurodegenerative Diseases," *Cold Spring Harbor perspectives in biology*, vol. 10, p. a033118, 2018.
- [112] C. Sato, N. R. Barthélemy, K. G. Mawuenyega, B. W. Patterson, B. A. Gordon, J. Jockel-Balsarotti, *et al.*, "Tau Kinetics in Neurons and the Human Central Nervous System," *Neuron*, vol. 97, pp. 1284-1298.e7, 2018/03/21/ 2018.
- [113] B. J. Hanseeuw, R. A. Betensky, H. I. L. Jacobs, A. P. Schultz, J. Sepulcre, J. A. Becker, *et al.*, "Association of Amyloid and Tau With Cognition in Preclinical Alzheimer Disease: A Longitudinal Study," *JAMA Neurology*, vol. 76, pp. 915-924, 2019.
- [114] M. J. Metcalfe and M. E. Figueiredo-Pereira, "Relationship between tau pathology and neuroinflammation in Alzheimer's disease," *Mt Sinai J Med*, vol. 77, pp. 50-8, Jan-Feb 2010.
- [115] M. Stoiljkovic, T. L. Horvath, and M. Hajós, "Therapy for Alzheimer's disease: Missing targets and functional markers?," *Ageing Research Reviews*, vol. 68, p. 101318, 2021/07/01/ 2021.
- [116] L. Buée, T. Bussièrre, V. Buée-Scherrer, A. Delacourte, and P. R. Hof, "Tau protein isoforms, phosphorylation and role in neurodegenerative disorders," *Brain Res Brain Res Rev*, vol. 33, pp. 95-130, Aug 2000.

- [117] P. Barbier, O. Zejneli, M. Martinho, A. Lasorsa, V. Belle, C. Smet-Nocca, *et al.*, "Role of Tau as a Microtubule-Associated Protein: Structural and Functional Aspects," *Front Aging Neurosci*, vol. 11, p. 204, 2019.
- [118] K. A. Butner and M. W. Kirschner, "Tau protein binds to microtubules through a flexible array of distributed weak sites," *Journal of Cell Biology*, vol. 115, pp. 717-730, 1991.
- [119] E. M. Mandelkow, J. Biernat, G. Drewes, N. Gustke, B. Trinczek, and E. Mandelkow, "Tau domains, phosphorylation, and interactions with microtubules," *Neurobiology of Aging*, vol. 16, pp. 355-362, 1995/05/01/ 1995.
- [120] M. Merezko, R. L. Uronen, and H. J. Huttunen, "The Cell Biology of Tau Secretion," *Front Mol Neurosci*, vol. 13, p. 569818, 2020.
- [121] C. H. Michel, S. Kumar, D. Pinotsi, A. Tunnacliffe, P. St George-Hyslop, E. Mandelkow, *et al.*, "Extracellular monomeric tau protein is sufficient to initiate the spread of tau protein pathology," *J Biol Chem*, vol. 289, pp. 956-67, Jan 10 2014.
- [122] M. Augusto-Oliveira, G. P. Arrifano, A. Lopes-Araújo, L. Santos-Sacramento, P. Y. Takeda, D. C. Anthony, *et al.*, "What Do Microglia Really Do in Healthy Adult Brain?," *Cells*, vol. 8, Oct 22 2019.
- [123] Dorothy P. Schafer, Emily K. Lehrman, Amanda G. Kautzman, R. Koyama, Alan R. Mardinly, R. Yamasaki, *et al.*, "Microglia Sculpt Postnatal Neural Circuits in an Activity and Complement-Dependent Manner," *Neuron*, vol. 74, pp. 691-705, 5/24/ 2012.
- [124] W. T. Wong, "Microglial aging in the healthy CNS: phenotypes, drivers, and rejuvenation," *Front Cell Neurosci*, vol. 7, p. 22, 2013.
- [125] R. von Bernhardi, F. Heredia, N. Salgado, and P. Muñoz, "Microglia Function in the Normal Brain," *Adv Exp Med Biol*, vol. 949, pp. 67-92, 2016.
- [126] T. L. Tay, J. C. Savage, C. W. Hui, K. Bisht, and M.-È. Tremblay, "Microglia across the lifespan: from origin to function in brain development, plasticity and cognition," *The Journal of Physiology*, vol. 595, pp. 1929-1945, 2017/03/15 2017.

- [127] S. Hickman, S. Izzy, P. Sen, L. Morsett, and J. El Khoury, "Microglia in neurodegeneration," *Nat Neurosci*, vol. 21, pp. 1359-1369, Oct 2018.
- [128] F. Ginhoux, S. Lim, G. Hoeffel, D. Low, and T. Huber, "Origin and differentiation of microglia," *Front Cell Neurosci*, vol. 7, p. 45, 2013.
- [129] Q. Li, Z. Cheng, L. Zhou, S. Darmanis, N. F. Neff, J. Okamoto, *et al.*, "Developmental Heterogeneity of Microglia and Brain Myeloid Cells Revealed by Deep Single-Cell RNA Sequencing," *Neuron*, vol. 101, pp. 207-223.e10, Jan 16 2019.
- [130] A. Witting, P. Müller, A. Herrmann, H. Kettenmann, and C. Nolte, "Phagocytic clearance of apoptotic neurons by Microglia/Brain macrophages in vitro: involvement of lectin-, integrin-, and phosphatidylserine-mediated recognition," *J Neurochem*, vol. 75, pp. 1060-70, Sep 2000.
- [131] D. Davalos, J. Grutzendler, G. Yang, J. V. Kim, Y. Zuo, S. Jung, *et al.*, "ATP mediates rapid microglial response to local brain injury in vivo," *Nat Neurosci*, vol. 8, pp. 752-758, 06//print 2005.
- [132] M. Nakanishi, T. Niidome, S. Matsuda, A. Akaike, T. Kihara, and H. Sugimoto, "Microglia-derived interleukin-6 and leukaemia inhibitory factor promote astrocytic differentiation of neural stem/progenitor cells," *Eur J Neurosci*, vol. 25, pp. 649-58, Feb 2007.
- [133] J. Aarum, K. Sandberg, S. L. Haeberlein, and M. A. Persson, "Migration and differentiation of neural precursor cells can be directed by microglia," *Proc Natl Acad Sci U S A*, vol. 100, pp. 15983-8, Dec 23 2003.
- [134] S.-H. Lim, E. Park, B. You, Y. Jung, A. R. Park, S. G. Park, *et al.*, "Neuronal Synapse Formation Induced by Microglia and Interleukin 10," *PLOS ONE*, vol. 8, p. e81218, 2013.
- [135] Y. Li, X. F. Du, C. S. Liu, Z. L. Wen, and J. L. Du, "Reciprocal regulation between resting microglial dynamics and neuronal activity in vivo," *Dev Cell*, vol. 23, pp. 1189-202, Dec 11 2012.

- [136] O. Butovsky, Y. Ziv, A. Schwartz, G. Landa, A. E. Talpalar, S. Pluchino, *et al.*, "Microglia activated by IL-4 or IFN-gamma differentially induce neurogenesis and oligodendrogenesis from adult stem/progenitor cells," *Mol Cell Neurosci*, vol. 31, pp. 149-60, Jan 2006.
- [137] R. C. Paolicelli, G. Bolasco, F. Pagani, L. Maggi, M. Scianni, P. Panzanelli, *et al.*, "Synaptic pruning by microglia is necessary for normal brain development," *Science*, vol. 333, pp. 1456-8, Sep 9 2011.
- [138] H. Keren-Shaul, A. Spinrad, A. Weiner, O. Matcovitch-Natan, R. Dvir-Szternfeld, T. K. Ulland, *et al.*, "A Unique Microglia Type Associated with Restricting Development of Alzheimer's Disease," *Cell*, vol. 169, pp. 1276-1290.e17, Jun 15 2017.
- [139] B. Zhang, C. Gaiteri, L.-G. Bodea, Z. Wang, J. McElwee, Alexei A. Podtelezchnikov, *et al.*, "Integrated Systems Approach Identifies Genetic Nodes and Networks in Late-Onset Alzheimer's Disease," *Cell*, vol. 153, pp. 707-720, 2013/04/25/ 2013.
- [140] C. E. G. Leyns and D. M. Holtzman, "Glial contributions to neurodegeneration in tauopathies," *Mol Neurodegener*, vol. 12, p. 50, Jun 29 2017.
- [141] S. E. Headland, H. R. Jones, A. S. V. D'Sa, M. Perretti, and L. V. Norling, "Cutting-Edge Analysis of Extracellular Microparticles using ImageStreamX Imaging Flow Cytometry," *Sci. Rep.*, vol. 4, 06/10/online 2014.
- [142] C. A. Juul, S. Grubb, K. A. Poulsen, T. Kyed, N. Hashem, I. H. Lambert, *et al.*, "Anoctamin 6 differs from VRAC and VSOAC but is involved in apoptosis and supports volume regulation in the presence of Ca<sup>2+</sup>," *Pflugers Arch*, vol. 466, pp. 1899-910, Oct 2014.
- [143] W. L. Beatty and D. G. Russell, "Identification of mycobacterial surface proteins released into subcellular compartments of infected macrophages," *Infect Immun*, vol. 68, pp. 6997-7002, Dec 2000.

- [144] C. Frehel, C. de Chastellier, T. Lang, and N. Rastogi, "Evidence for inhibition of fusion of lysosomal and prelysosomal compartments with phagosomes in macrophages infected with pathogenic *Mycobacterium avium*," *Infect Immun*, vol. 52, pp. 252-62, Apr 1986.
- [145] F. G. Ortega, M. T. Roefs, D. de Miguel Perez, S. A. Kooijmans, O. G. de Jong, J. P. Sluijter, *et al.*, "Interfering with endolysosomal trafficking enhances release of bioactive exosomes," *Nanomedicine: Nanotechnology, Biology and Medicine*, vol. 20, p. 102014, 2019/08/01/ 2019.
- [146] D. Lagadic-Gossmann, L. Huc, and V. Lecreur, "Alterations of intracellular pH homeostasis in apoptosis: origins and roles," *Cell Death & Differentiation*, vol. 11, pp. 953-961, 2004/09/01 2004.
- [147] G. van Niel, G. D'Angelo, and G. Raposo, "Shedding light on the cell biology of extracellular vesicles," *Nat Rev Mol Cell Biol*, vol. 19, pp. 213-228, Apr 2018.
- [148] M. Yáñez-Mó, P. R. Siljander, Z. Andreu, A. B. Zavec, F. E. Borràs, E. I. Buzas, *et al.*, "Biological properties of extracellular vesicles and their physiological functions," *J Extracell Vesicles*, vol. 4, p. 27066, 2015.
- [149] H. Pollet, L. Conrard, A. S. Cloos, and D. Tyteca, "Plasma Membrane Lipid Domains as Platforms for Vesicle Biogenesis and Shedding?," *Biomolecules*, vol. 8, Sep 14 2018.
- [150] M. L. Kirsten, R. A. Baron, M. C. Seabra, and O. Ces, "Rab1a and Rab5a preferentially bind to binary lipid compositions with higher stored curvature elastic energy," *Mol Membr Biol*, vol. 30, pp. 303-14, Jul 2013.
- [151] C. McDonald, G. Jovanovic, O. Ces, and M. Buck, "Membrane Stored Curvature Elastic Stress Modulates Recruitment of Maintenance Proteins PspA and Vipp1," *MBio*, vol. 6, pp. e01188-15, 2015.
- [152] B. Stancevic and R. Kolesnick, "Ceramide-rich platforms in transmembrane signaling," *FEBS Lett*, vol. 584, pp. 1728-40, May 3 2010.

- [153] J. M. Holopainen, M. I. Angelova, and P. K. Kinnunen, "Vectorial budding of vesicles by asymmetrical enzymatic formation of ceramide in giant liposomes," *Biophys J*, vol. 78, pp. 830-8, Feb 2000.
- [154] K. Trajkovic, C. Hsu, S. Chiantia, L. Rajendran, D. Wenzel, F. Wieland, *et al.*, "Ceramide triggers budding of exosome vesicles into multivesicular endosomes," *Science*, vol. 319, pp. 1244-7, Feb 29 2008.
- [155] C. Subra, K. Laulagnier, B. Perret, and M. Record, "Exosome lipidomics unravels lipid sorting at the level of multivesicular bodies," *Biochimie*, vol. 89, pp. 205-12, Feb 2007.
- [156] F. M. Goni and A. Alonso, "Biophysics of sphingolipids I. Membrane properties of sphingosine, ceramides and other simple sphingolipids," *Biochim Biophys Acta*, vol. 1758, pp. 1902-21, Dec 2006.
- [157] A. D. Tepper, P. Ruurs, T. Wiedmer, P. J. Sims, J. Borst, and W. J. van Blitterswijk, "Sphingomyelin hydrolysis to ceramide during the execution phase of apoptosis results from phospholipid scrambling and alters cell-surface morphology," *J Cell Biol*, vol. 150, pp. 155-64, Jul 10 2000.
- [158] J. Huotari and A. Helenius, "Endosome maturation," *Embo j*, vol. 30, pp. 3481-500, Aug 31 2011.
- [159] J. P. Luzio, M. D. Parkinson, S. R. Gray, and N. A. Bright, "The delivery of endocytosed cargo to lysosomes," *Biochem Soc Trans*, vol. 37, pp. 1019-21, Oct 2009.
- [160] H. Braak and E. Braak, "Staging of Alzheimer's disease-related neurofibrillary changes," *Neurobiol Aging*, vol. 16, pp. 271-8; discussion 278-84, May-Jun 1995.
- [161] J. L. Jankowsky and H. Zheng, "Practical considerations for choosing a mouse model of Alzheimer's disease," *Molecular neurodegeneration*, vol. 12, pp. 89-89, 2017.
- [162] Y. Yoshiyama, M. Higuchi, B. Zhang, S. M. Huang, N. Iwata, T. C. Saido, *et al.*, "Synapse loss and microglial activation precede tangles in a P301S tauopathy mouse model," *Neuron*, vol. 53, pp. 337-51, Feb 1 2007.

- [163] C. A. Lasagna-Reeves, M. de Haro, S. Hao, J. Park, M. W. Rousseaux, I. Al-Ramahi, *et al.*, "Reduction of Nuak1 Decreases Tau and Reverses Phenotypes in a Tauopathy Mouse Model," *Neuron*, vol. 92, pp. 407-418, Oct 19 2016.
- [164] H. Takeuchi, M. Iba, H. Inoue, M. Higuchi, K. Takao, K. Tsukita, *et al.*, "P301S mutant human tau transgenic mice manifest early symptoms of human tauopathies with dementia and altered sensorimotor gating," *PLoS One*, vol. 6, p. e21050, 2011.
- [165] M. Maruyama, H. Shimada, T. Suhara, H. Shinotoh, B. Ji, J. Maeda, *et al.*, "Imaging of tau pathology in a tauopathy mouse model and in Alzheimer patients compared to normal controls," *Neuron*, vol. 79, pp. 1094-108, Sep 18 2013.
- [166] M. Iba, J. L. Guo, J. D. McBride, B. Zhang, J. Q. Trojanowski, and V. M. Lee, "Synthetic tau fibrils mediate transmission of neurofibrillary tangles in a transgenic mouse model of Alzheimer's-like tauopathy," *J Neurosci*, vol. 33, pp. 1024-37, Jan 16 2013.
- [167] B. Zhang, J. Carroll, J. Q. Trojanowski, Y. Yao, M. Iba, J. S. Potuzak, *et al.*, "The microtubule-stabilizing agent, epothilone D, reduces axonal dysfunction, neurotoxicity, cognitive deficits, and Alzheimer-like pathology in an interventional study with aged tau transgenic mice," *J Neurosci*, vol. 32, pp. 3601-11, Mar 14 2012.
- [168] X. Chai, J. L. Dage, and M. Citron, "Constitutive secretion of tau protein by an unconventional mechanism," *Neurobiol Dis*, vol. 48, pp. 356-66, Dec 2012.
- [169] Y. Wang, V. Balaji, S. Kaniyappan, L. Krüger, S. Irsen, K. Tepper, *et al.*, "The release and trans-synaptic transmission of Tau via exosomes," *Mol Neurodegener*, vol. 12, p. 5, Jan 13 2017.
- [170] C. Pernègre, A. Duquette, and N. Leclerc, "Tau Secretion: Good and Bad for Neurons," *Front Neurosci*, vol. 13, p. 649, 2019.
- [171] P. Spitzer, L. M. Mulzer, T. J. Oberstein, L. E. Munoz, P. Lewczuk, J. Kornhuber, *et al.*, "Microvesicles from cerebrospinal fluid of patients with Alzheimer's disease display reduced concentrations of tau and APP protein," *Sci Rep*, vol. 9, p. 7089, May 8 2019.



- [172] S. Yona, K.-W. Kim, Y. Wolf, A. Mildner, D. Varol, M. Breker, *et al.*, "Fate Mapping Reveals Origins and Dynamics of Monocytes and Tissue Macrophages under Homeostasis," *Immunity*, vol. 38, pp. 79-91, 2013.
- [173] E. F. Willis, P. F. Bartlett, and J. Vukovic, "Protocol for Short- and Longer-term Spatial Learning and Memory in Mice," *Frontiers in Behavioral Neuroscience*, vol. 11, 2017-October-17 2017.
- [174] J. Brelstaff, A. M. Tolkovsky, B. Ghetti, M. Goedert, and M. G. Spillantini, "Living Neurons with Tau Filaments Aberrantly Expose Phosphatidylserine and Are Phagocytosed by Microglia," *Cell Rep*, vol. 24, pp. 1939-1948.e4, Aug 21 2018.
- [175] G. C. Brown and J. J. Neher, "Eaten alive! Cell death by primary phagocytosis: 'phagoptosis'," *Trends in Biochemical Sciences*, vol. 37, pp. 325-332, 2012/08/01/ 2012.
- [176] S. Wakselman, C. Béchade, A. Roumier, D. Bernard, A. Triller, and A. Bessis, "Developmental Neuronal Death in Hippocampus Requires the Microglial CD11b Integrin and DAP12 Immunoreceptor," *The Journal of Neuroscience*, vol. 28, p. 8138, 2008.
- [177] J. L. Marín-Teva, I. Dusart, C. Colin, A. Gervais, N. van Rooijen, and M. Mallat, "Microglia Promote the Death of Developing Purkinje Cells," *Neuron*, vol. 41, pp. 535-547, 2004/02/19/ 2004.
- [178] S. Amor, F. Puentes, D. Baker, and P. van der Valk, "Inflammation in neurodegenerative diseases," *Immunology*, vol. 129, pp. 154-69, Feb 2010.
- [179] M. Fricker, J. J. Neher, J. W. Zhao, C. Théry, A. M. Tolkovsky, and G. C. Brown, "MFG-E8 mediates primary phagocytosis of viable neurons during neuroinflammation," *J Neurosci*, vol. 32, pp. 2657-66, Feb 22 2012.
- [180] J. J. Neher, U. Neniskyte, J. W. Zhao, A. Bal-Price, A. M. Tolkovsky, and G. C. Brown, "Inhibition of microglial phagocytosis is sufficient to prevent inflammatory neuronal death," *J Immunol*, vol. 186, pp. 4973-83, Apr 15 2011.

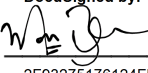
- [181] A. C. Doran, A. Yurdagul, Jr., and I. Tabas, "Efferocytosis in health and disease," *Nat Rev Immunol*, vol. 20, pp. 254-267, Apr 2020.
- [182] U. Neniskyte, J. J. Neher, and G. C. Brown, "Neuronal death induced by nanomolar amyloid  $\beta$  is mediated by primary phagocytosis of neurons by microglia," *J Biol Chem*, vol. 286, pp. 39904-13, Nov 18 2011.
- [183] A. Görlach, K. Bertram, S. Hudecova, and O. Krizanova, "Calcium and ROS: A mutual interplay," *Redox Biol*, vol. 6, pp. 260-271, Dec 2015.
- [184] C. Hidalgo, R. Bull, M. I. Behrens, and P. Donoso, "Redox regulation of RyR-mediated  $\text{Ca}^{2+}$  release in muscle and neurons," *Biol Res*, vol. 37, pp. 539-52, 2004.
- [185] H.-J. Chen-Engerer, J. Hartmann, R. M. Karl, J. Yang, S. Feske, and A. Konnerth, "Two types of functionally distinct  $\text{Ca}^{2+}$  stores in hippocampal neurons," *Nature Communications*, vol. 10, p. 3223, 2019/07/19 2019.
- [186] K. Furukawa, Y. Wang, P. J. Yao, W. Fu, M. P. Mattson, Y. Itoyama, *et al.*, "Alteration in calcium channel properties is responsible for the neurotoxic action of a familial frontotemporal dementia tau mutation," *J Neurochem*, vol. 87, pp. 427-36, Oct 2003.
- [187] Q. Wu, Y. Bai, W. Li, E. E. Congdon, W. Liu, Y. Lin, *et al.*, "Increased neuronal activity in motor cortex reveals prominent calcium dyshomeostasis in tauopathy mice," *Neurobiol Dis*, vol. 147, p. 105165, Jan 2021.
- [188] J. Ye, Y. Yin, Y. Yin, H. Zhang, H. Wan, L. Wang, *et al.*, "Tau-induced upregulation of C/EBP $\beta$ -TRPC1-SOCE signaling aggravates tauopathies: A vicious cycle in Alzheimer neurodegeneration," *Aging Cell*, vol. 19, p. e13209, Sep 2020.
- [189] J. Lewis, E. McGowan, J. Rockwood, H. Melrose, P. Nacharaju, M. Van Slegtenhorst, *et al.*, "Neurofibrillary tangles, amyotrophy and progressive motor disturbance in mice expressing mutant (P301L) tau protein," *Nat Genet*, vol. 25, pp. 402-5, Aug 2000.
- [190] F. Simões, J. Ousingawat, P. Wanitchakool, A. Fonseca, I. Cabrita, R. Benedetto, *et al.*, "CFTR supports cell death through ROS-dependent activation of TMEM16F

- (anoctamin 6)," *Pflügers Archiv - European Journal of Physiology*, vol. 470, pp. 305-314, 2018/02/01 2018.
- [191] S. Dujardin, S. Bégard, R. Caillierez, C. Lachaud, L. Delattre, S. Carrier, *et al.*, "Ectosomes: a new mechanism for non-exosomal secretion of tau protein," *PLoS One*, vol. 9, p. e100760, 2014.
- [192] Y. Fang, N. Wu, X. Gan, W. Yan, J. C. Morrell, and S. J. Gould, "Higher-order oligomerization targets plasma membrane proteins and HIV gag to exosomes," *PLoS Biol*, vol. 5, p. e158, Jun 2007.
- [193] C. Tricarico, J. Clancy, and C. D'Souza-Schorey, "Biology and biogenesis of shed microvesicles," *Small GTPases*, vol. 8, pp. 220-232, Oct 2 2017.

## Publishing Agreement

It is the policy of the University to encourage open access and broad distribution of all theses, dissertations, and manuscripts. The Graduate Division will facilitate the distribution of UCSF theses, dissertations, and manuscripts to the UCSF Library for open access and distribution. UCSF will make such theses, dissertations, and manuscripts accessible to the public and will take reasonable steps to preserve these works in perpetuity.

I hereby grant the non-exclusive, perpetual right to The Regents of the University of California to reproduce, publicly display, distribute, preserve, and publish copies of my thesis, dissertation, or manuscript in any form or media, now existing or later derived, including access online for teaching, research, and public service purposes.

DocuSigned by:  
  
2F93275176124FB... Author Signature

3/22/2021  
Date